Communications
Research Centre
Centre de recherches
sur les communications

Analysis and Experiments on the Frequency-Independent Strong-Signal Suppressor (FISSS)

by

David Sychaleum, E. Barry Felstead and Gilbert A. Morin

IC

CRC REPORT NO. 98-006

November 1998
Ottawa

TK
5102.5
C673e
#98-006

Industry Canada Industrie Canada

This work was supported by the Canadian Department of National Defence through the Defence Research and Development Branch.

Canada

IC
SIC2.5
C673e
498-006
c.b
S-Gen

Analysis and Experiments on the Frequency-Independent Strong-Signal Suppressor (FISSS)

by

David Sychaleum, E. Barry Felstead
DMSCP/MILSATCOM
Communications Research Centre

and

Gilbert A. Morin
SST/MILSATCOM
Defence Research Establishment Ottawa

Industry Canada
Library - Queen
AOUT AUG 2 2 2012
Industrie Canada
Bibliothèque - Queen

CRC LIBRARY
-01- 2 2 1999
BIBLIOTHEQUE CRC

This work was supported by the Canadian Department of National Defence through the Defence Research and Development Branch.

INDUSTRY CANADA
CRC REPORT NO. 98-006

Canada

November 1998
Ottawa

ABSTRACT

The frequency-independent strong-signal suppressor (FISSS) uses nonlinear processing plus cancellation techniques to provide substantial interference suppression. However, only laboratory proof of its operation existed. Although considerable effort went into trying to determine the principle of operation, this principle was not found. In this report, some analytical and simulation attacks on this problem are described. Extensive laboratory measurements were made on devices operating at 1.5 GHz and 10 GHz. The 10 GHz device was combined with direct-sequence spread spectrum, and had measured processing gains of about 12 dB against CW and frequency-modulated single tones. The experimental highlight was the successful suppression of noise interference of between 6 and 12 dB, depending upon the noise bandwidth.

RÉSUMÉ

Le suppresseur de signaux forts indépendant de la fréquence (FISSS) utilise le conditionnement nonlinéaire associé à des techniques d'élimination de signaux pour obtenir une suppression d'interférence substantielle. Cependant, il n'existait, jusqu'à maintenant que des preuves expérimentales de son opération. Beaucoup d'efforts ont été fournis pour déterminer son principe d'opération mais sans grand succès. Dans le présent rapport, le problème est analysé du point de vue analytique et numérique. Des mesures extensives de laboratoire furent conduites sur plusieurs unités FISSS à des fréquences de 1.5 et 10 GHz. L'unité de 10 GHz a été évaluée avec un signal à spectre dispersé en séquence directe. On a ainsi démontré un gain résultant du traitement d'environ 12 dB contre un brouilleur en signal continu ou modulé en fréquence. Les résultats les plus surprenants furent cependant obtenus par la suppression d'un brouilleur à bruit de 6 à 12 dB dépendant de la bande passante du bruit.

EXECUTIVE SUMMARY

Interference suppression techniques are of considerable interest in military radio communications. The two traditional approaches are spread-spectrum and antenna spatial techniques. In addition, there are a number of auxiliary interference-suppression techniques that have the potential of providing extra protection from interference. As military radio communications systems require ever increasing information bandwidths, the protection afforded by spread spectrum decreases proportionally. Therefore, auxiliary interference-suppression techniques could play an important role in making up for the decreased spread-spectrum protection, thereby allowing for higher data rates.

One such auxiliary interference-suppression technique is the frequency-independent strong-signal suppressor (FISSS), which is the subject of this report. The FISSS is a nonlinear solid-state device that is placed after the antenna. It has been found in the lab that the FISSS can provide significant interference suppression for a variety of interference waveforms. For example, one 10-GHz FISSS device, protecting a direct-sequence spread-spectrum signal, displayed measured processing gains of about 12 dB against CW and frequency-modulated single tones. The experimental highlight was the successful suppression of noise interference of 6 to 12 dB, depending on the noise bandwidth.

Despite these early and continued experimental successes, the progress in understanding the FISSS has been dogged by a number of problems. One problem is that no theory had been developed to explain its operation. Therefore, it was difficult to design and optimize new devices. A second problem is that its performance had not been fully measured, characterized, and recorded, especially for types of interference other than CW tones. A third problem arises because of the nonlinearities in the FISSS that cause intermodulation (IM) products thereby degrading performance.

This report documents the effort made to overcome the problems listed above. Included in this effort was construction of devices operating at frequencies of 1.5 GHz and 10 GHz. The progress includes some inroads in the theory, thorough measurement of several devices, some means of minimizing the effects of the intermodulation, and demonstration of noise interference suppression. Although considerable progress was made, some key problem areas remained unresolved.

TABLE OF CONTENTS

1. INTRODUCTION

Interference suppression techniques are of considerable interest in military radio communications. The two traditional approaches are spread-spectrum, and antenna spatial techniques. In addition, there are a number of auxiliary interference-suppression techniques that have the potential of providing extra protection from interference. As military systems require ever increasing information bandwidths, the protection afforded by spread spectrum decreases proportionally. Therefore, auxiliary interference-suppression techniques could play an important role in making up for the decreased processing gain of spread spectrum.

One such auxiliary interference-suppression technique is the frequency-independent strong-signal suppressor (FISSS), which is the subject of this report. The FISSS is a nonlinear solid-state device that is placed after the receive antenna. It is based upon the microwave halver, and has an amplitude-dependent voltage standing-wave ratio that exhibits a sharp transition from matched load to open load. Signals having amplitudes greater than a predetermined threshold (e.g. the interfering signals) are absorbed while weaker signals (e.g. the desired signal) are reflected and extracted by means of a directional coupler or circulator. It has been found in the lab that the FISSS can provide significant interference suppression for a variety of interference waveforms. The FISSS does not depend on the frequency of the interfering signal, but rather upon its amplitude relative to the desired signal.

Historically, the action of the FISSS was discovered by happenstance at a Canadian company, Telemus Corporation. The amplitude-dependent return loss of the microwave halver, as invented at DREO, was observed. It was thought that this characteristic could be used to suppress strong signals relative to combined small signals. Early work on the use of the FISSS for direct-sequence spread signals was supported under a contract from DND through the Chief of Research and Development with Brian W. Kozminchuk as the Scientific Authority. Some of these results were reported in [1] and [2]. The resulting patent, [3], was retained by the inventor. When parts of Telemus were taken over by CAL Corporation, it was necessary for CAL to obtain the intellectual property (IP) directly from the inventor. A contract was given to CAL by DND to develop and deliver a FISSS operating at 10 GHz and an associated test bed [4]. Certain results on that FISSS will be reported here. Later, the IP for the FISSS was spun off to Omega Corporation. The current status of Omega and the IP are not known to the authors.

In the early work [1], it was shown that the FISSS could enhance the performance of direct-sequence (DS) spread-spectrum (SS) signals by tens of dB for CW or swept-frequency single-tone interference. Later, enhancement of performance of these same signals by 6 to 12 dB was measured against white Gaussian noise interference [5]. Despite these early successes, the progress of the FISSS has been dogged by a number of problems. One problem is that no theory had been developed to explain its operation. Therefore, it was difficult to design and optimize new devices. A second problem is that its performance had not been fully measured, characterized, and recorded, especially for forms of interference other than CW tones. A third problem arises because of the nonlinearities in the FISSS that cause intermodulation (IM) products thereby degrading performance.

This report documents the effort made to overcome the problems listed above. Included in this effort was construction of devices operating at frequencies of 1.5 GHz and at 10 GHz. The progress includes some inroads in the theory, thorough measurement of several devices, some means of minimizing the effects of the intermodulation, and demonstration of noise-interference suppression. Although considerable progress was made, some key problem areas remained unresolved.

2. AUXILIARY INTERFERENCE SUPPRESSION TECHNIQUES — GENERAL

2.1 BACKGROUND ON INTERFERENCE SUPPRESSION METHODS

Radio receivers can suffer from a wide variety of interference including intentional jamming, unintentional radio frequency interference (RFI), and passive intermodulation product (PIM). Since the early days of radio, much work has gone into trying to mitigate the effects of interference. Two prominent approaches to combating interference are the use of spread spectrum techniques, and antenna spatial techniques. Simple antenna spatial techniques have been used almost since the beginning of radio and involve taking advantage of any directionality of antenna patterns. Spread spectrum was originally developed for military use in the presence of strong jamming. Currently, it is widely used in a variety of applications that suffer from interference including the interference from other users of the same system.

A generic radio receiver using both techniques is illustrated in Fig. 1. Two forms of antenna spatial techniques are shown: low sidelobe antennas, and nulling. A processing gain can be defined for this process. For the low sidelobe method $PG_{ant} \approx G_S / G_I$ where G_S is the gain toward the signal source and G_I is the sidelobe gain toward the interference. For nulling, $PG_{ant} \approx$ null depth relative to G_S. A current hot topic is for commercial cellular radio in which "smart antennas" are used to separate mobile users by methods borrowed from nulling. For the spread spectrum, a processing gain is sometimes defined as $PG_{ss} \approx W_{ss}/R_b$ where W_{ss} is the spread bandwidth and R_b is the information bit rate. If the signal-to-noise-plus-interference ratio ($SNIR$) at the antenna aperture is $S/(N+I)$, then conceptually, the antenna processing gain results in an increased SNIR $\approx S/(N+I/PG_{ant})$. The spread spectrum further increases the SNIR to $\approx S/\left[N+I/(PG_{ant}+PG_{ss})\right]$.

There are a number of other interference suppression techniques that can be used as an auxiliary to the two main techniques and, in some cases, for stand-alone suppression. An overview of such techniques is found in [6]. A brief overview of these techniques is given below before discussing the FISSS specifically.

There is a push in military radio systems for ever-increasing data rates and, therefore, increasing bandwidths. However, as the information bandwidth, approximately R_b, increases, the spread-spectrum processing gain, $PG_{ss} \approx W_{ss}/R_b$, correspondingly decreases. Auxiliary interference suppression techniques can potentially be used to compensate for this decrease.

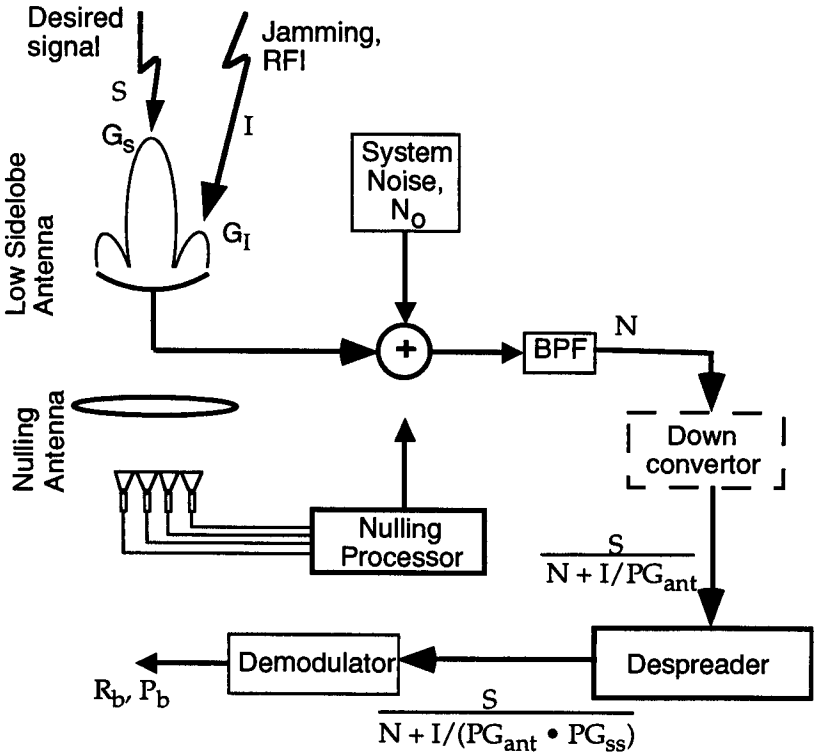

Fig. 1. A conceptual block diagram of a wireless receiver using both antenna-spatial and spread-spectrum techniques to combat interference.

2.2 Desired Features of Auxiliary Suppression Techniques

There are a number of features that auxiliary suppression techniques should possess in addition to having a good processing gain, PG_{aux}. First, it should not introduce degradations such as intermodulation or increased noise figure that are worse than the original interference. Secondly, it should be economical to implement. Thirdly, it should be complementary to other techniques of combating interference so that the total processing gain is, in dB, just the sum of the individual processing gains:

$$PG_{total}|_{dB} = PG_{ant}|_{dB} + PG_{ss}|_{dB} + PG_{aux}|_{dB} \tag{1}$$

Finally, for combating intelligent jamming, auxiliary methods must be capable of functioning well under a variety of jamming strategies.

2.3 Classification of Auxiliary Suppression Techniques

There are a wide variety of supplementary interference suppression techniques. The following attempts to put them into categories. The listing of categories and

types within each category are not exhaustive. The following classification relates primarily to where the interference suppression device fits in the receiver system. In some simpler cases of unintentional interference, the interference can be suppressed by rather simple, custom designed techniques such as narrow–band filtering. These simple techniques are not listed here. Also not included here are diversity (time, frequency, polarization, etc.) techniques that can be used to improve performance. The classification summary is as follows:

A. Frequency Dependent Auxiliary Techniques
   - Transversal filter
     - Linear [7]
     - Nonlinear [8]
   - Frequency filter
     - Linear [7]
     - Nonlinear [9]

B. Amplitude Dependent Auxiliary Techniques
   - Baseband Nonlinear Suppressors [10]
   - RF Nonlinear Suppressors
     - Nonlinearity alone[11], [12]
     - Nonlinearity plus subtraction [13], [14]

A summary of these topics is given in the next two sections.

2.4 Frequency Dependent Auxiliary Techniques

The frequency dependent category of auxiliary techniques operates on differences in frequency structure between the desired signal and the interference. In Fig. 2 is shown a generic form. The frequency dependent processor is shown located after the down converter but may be located elsewhere. The frequency dependent processor defines the type of frequency-dependent suppressor. The processor takes the form of a transversal filter in one type. For the frequency filter type, the processor can be as simple as an adjustable notch filter. More often, it takes the form of, in order, a Fourier transform, a selective removal or attenuation of certain frequency component, and an inverse transform. The transforms are often done with FFT algorithms.

For obvious reasons, the frequency dependent suppressors are best suited to combating signals with bandwidths much smaller than the desired signal. For

supporting spread-spectrum signals, they are of value primarily to direct-sequence (DS) systems. They are not of much value to frequency hopped (FH) systems since FH is inherently tolerant of narrow-band interference.

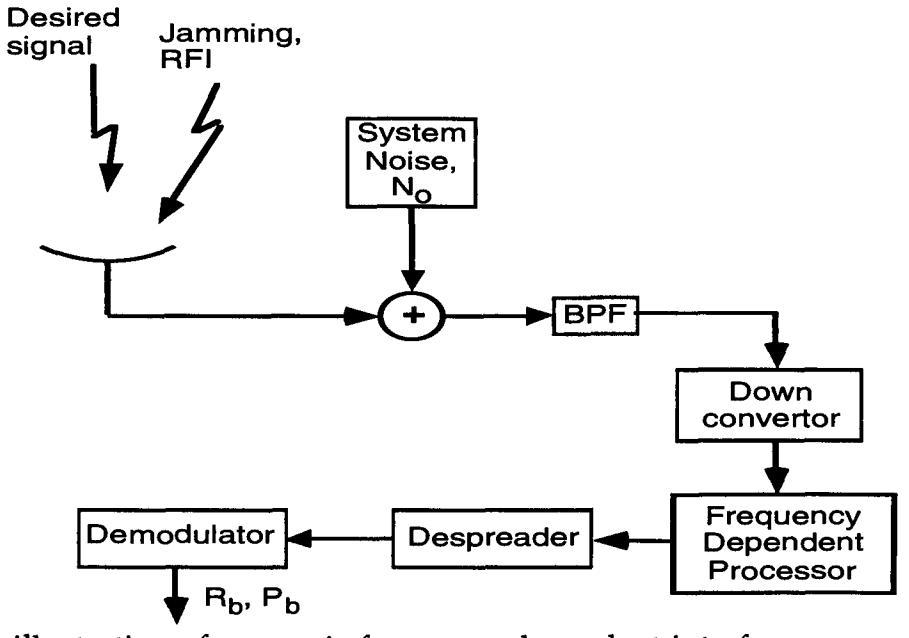

Fig. 2. An illustration of a generic frequency-dependent interference suppressor.

2.5 Amplitude Dependent Auxiliary Techniques

The base band nonlinear form of amplitude-dependent auxiliary interference suppressors generally use A/D converters after down conversion to base band [10]. Then, a variety of nonlinearities can be applied. In practice, the procedure of using a low number of bits along with variable quantization levels in the A/D conversion becomes the actual nonlinearity. There are similarities to the suppressors operating at RF. Since the FISSS operates at RF, we will not dwell on the base band forms.

3. FISSS DESCRIPTION

3.1 SIMPLIFIED DESCRIPTION

The simplified block diagram generally used (see [1], and [5]) to describe the operation of the basic FISSS is shown in Fig. 3. As shown, the FISSS operates at RF but could also be employed at IF. The input is assumed to consist of a weak desired signal combined with strong interfering signals, both with frequencies in the region of f_{in}. These signals go through a directional coupler or circulator to a nonlinear device. This device is primarily a microwave halver [15] but without the need to have an output port at $f_{in}/2$. The halver unit consists of a microstrip matching section and two varactor diodes. A DC bias sets the operating point of the diodes. In principle, the large interference has most of its energy converted to energy at frequencies around $f_{in}/2$. However, much of the small desired signal is not converted and is mismatched to the halver in such a way that it is mostly reflected. This reflected signal plus the reduced interference is obtained at the third port of the circulator.

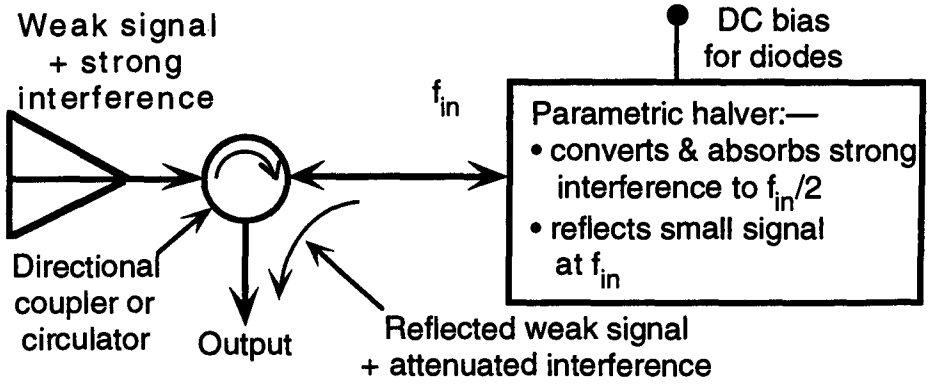

Fig. 3. Simplified block diagram of FISSS operation at the front end of a receiver.

3.2 SIMPLE EQUIVALENT CIRCUIT OF HALVER SECTION

A simplified equivalent circuit for the halver section is shown in Fig. 4. In turn, the equivalent circuit of a diode is shown at the right. It consists of 4 components: A nonlinear resistor (NLR), a series resistance, R_s, a nonlinear depletion capacitance, C_{depl}, and a nonlinear diffusion capacitance, C_{dif}. These three nonlinearities can be described, respectively, by:

$$I = I_s\left[\exp\left(qV/nkT\right)-1\right] \tag{2}$$

$$C_{dif} = \frac{t_T I_s q}{nkT} \exp\left(qV/nkT\right) \tag{3}$$

$$C_{depl} = C_{j0}\left(1 - V/V_j\right)^{-M} \tag{4}$$

where

I = current in the loop
I_s = saturation current through the NLR
t_T = forward transit time
C_{j0} = junction capacitance at 0 bias
V = junction voltage
V_j = junction potential
M = a constant, typically 0.5 for varactors and 0.33 for normal diodes
T = junction temperature, K
q = electronic charge
k = Boltzmann's constant
n = ideality factor, e.g. =1.84 for 1N4148 diode

The value of inductance is chosen so that the circuit would resonate in the sub-harmonic band around $f_{in}/2$ if the capacitance values in the diodes were at their DC bias values.

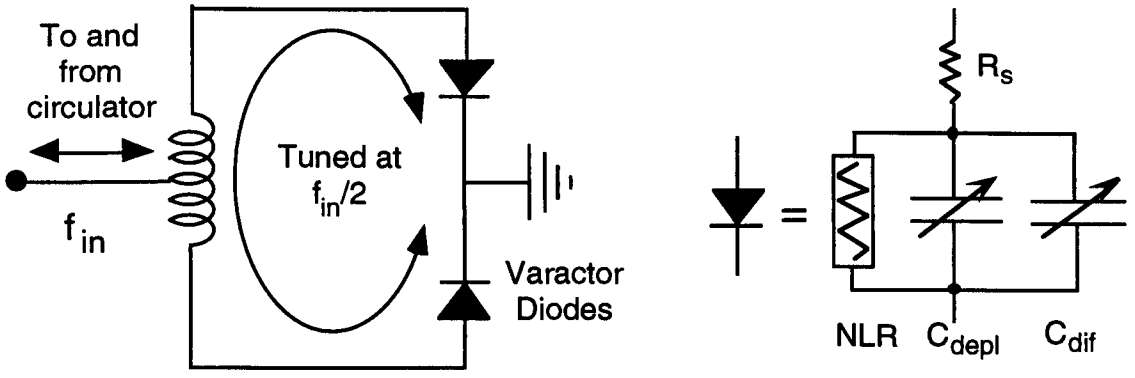

Fig. 4. Simplified equivalent circuit of main section of the FISSS. NLR = non-linear resistor, C_{depl} = depletion capacitance, C_{dif} = diffusion capacitance, and R_s = series resistance. The DC biasing circuit for the diodes is not shown.

Nonlinear interference-suppression devices such as the Smart AGC [11], and the dead-zone limiter [12] are notoriously difficult to analyze. These devices are *memoryless* and have a single nonlinearity. Conversely, the full circuit of Fig. 4 not

only has a memoryless nonlinearity, the NLR, it has memory through both the inductance and the capacitance, and, worse yet, it has two nonlinear capacitors. Therefore, analysis can be correspondingly more difficult. Nonetheless, some inroads have been made in developing analytical tools. It was discovered that a somewhat simpler circuit could be used to perform halving that results in simpler analysis. It was thought that if analysis techniques could be developed for this simpler circuit, then later they could be extended to the actual circuit. This simpler halver circuit is described in the next Chapter.

3.3 SUBTRACTION EFFECTS

Arnstein [16], in studying the results of Gagnon [2] on the FISSS, noted some similarities to the method developed by Baier and Friederichs [17], and then hypothesized that the FISSS circuit utilizes "a coherent subtraction approach." This astute observation was made without knowledge of the following two points. As shown in Fig. 5, the standard set up for the FISSS uses a variable phase shifter that is adjusted to get the maximum suppression. Furthermore, it is known that the circulator has leakage through the circulator to the output at a level of about –20 dB below the input signal, and it was thought that the large signal reflected from the main FISSS device is attenuated by about 20 dB. Suppressions of the strong signal of up to 40 dB had been achieved, yet the circulator allows a –20 dB signal to leak into the output. Therefore, it would be unlikely to achieve a strong signal suppression of >20 dB without the use of subtraction just as Arnstein surmised. Some experimental exploration of subtraction effects in the FISSS are discussed in a later chapter.

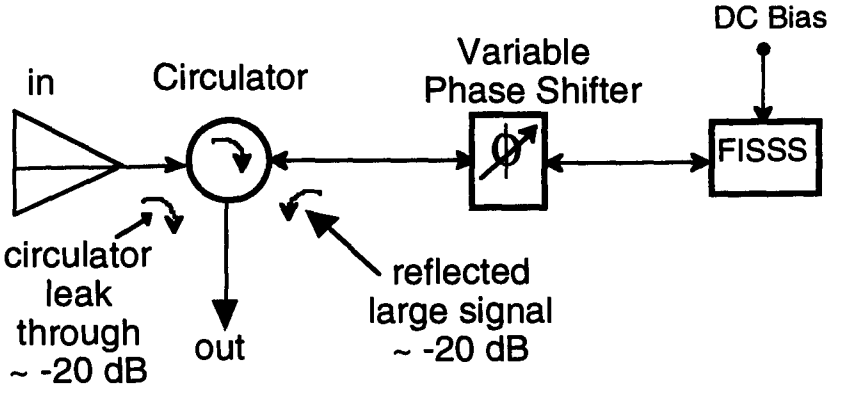

Fig. 5. FISSS circuitry with circulator leak through and phase adjuster shown.

4. ANALYSIS AND SIMULATION RELATED TO HALVERS

4.1 INTRODUCTION

The heart of the FISSS is the non-linear circuit that is based upon the halver. It was thought useful to see if the halver could be analyzed as a separate unit so that this analysis could in turn be applied to the complete FISSS. Furthermore, it was found that a halver could be implemented by a simpler circuit than was used in implementation of the FISSS. Below, this simple implementation of the halver is considered first. The circuit is described and an attempt is made at analysis. Then simulations, and implementation of a lumped-element version are described. Finally, a more complex microwave-halver circuit analysis is discussed.

4.2 BIFURCATION AND CHAOS AND THE R-L-DIODE HALVER

There are a number of circuits that exhibit period doubling which is also called "bifurcation" [18]. It turns out that in many of these circuits, the period doubling is a prelude to chaotic behaviour. One of the best examples of driven period-doubling circuits is the R-L-diode shown in Fig. 6. Ordinary diodes suffice for this circuit to work; varactors are not needed. No biasing is needed. The model of the diode itself is shown in Fig. 4. The value of L is chosen so that it resonates at $f_{in}/2$ with the zero-bias capacitance of the diode. For low values on the drive voltage, v_{ac}, the circuit behaves in the standard manner with components at f_{in} and its harmonics. However, above a certain value of v_{ac}, a subharmonic at $f_{in}/2$ suddenly appears, i.e., the period is doubled. As v_{ac} is increased further, there are further period increases, and eventually chaotic operation occurs. Here, we are primarily interested in only the first bifurcation. It is seen that the circuit in Fig. 6. has much in common with the FISSS circuit of Fig. 4, so that analysis for the simple circuit should be instructive for understanding the FISSS circuit.

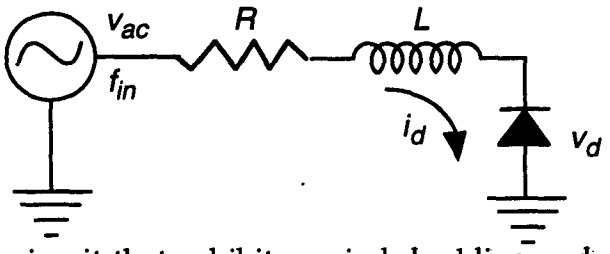

Fig. 6. The R-L-diode circuit that exhibits period doubling and chaotic behaviour.

4.3 ANALYSIS OF THE R-L-DIODE HALVER

4.3.1 The Role of the Exponential Function

Analysis of the circuit in Fig. 6 can be done with differential equations in the standard manner. However, the equivalent circuit of the diode, shown in Fig. 4, has an NLR, and two nonlinear capacitances. Therefore, parameters of the forms (2), (3), and (4) must be included in these equations. The fact that two of the forms involve exponentials has some useful aspects. First, the derivatives with respect to the diode voltage, v_d, are all also exponential. Therefore, all the following comments also apply to the derivatives. Secondly, when the diode voltage has the form

$$v_{ac}\cos(\theta),$$

then the resulting exponential can be expanded using the Jacobi-Anger formula:

$$\begin{aligned}\exp\left(\frac{qv_{ac}\cos(\theta)}{nkT}\right) &= \exp\left(C_1 v_{ac}\cos(\theta)\right) \\ &= I_0(C_1 v_{ac}) + \sum_{m=1}^{\infty} I_m(C_1 v_{ac})\cos(m\theta)\end{aligned} \tag{5}$$

where $I_m(\,)$ is the modified Bessel function of the first kind and order m, and C_1 is a constant. Typically, θ has the form $\theta = 2\pi ft + \phi$. The expansion (5) can be examined for only the harmonics of interest thereby generating exact values. Furthermore, (5) can be used for expanding the products of these exponentials, which is useful technique when the voltage is the sum of sinusoids.

A further analysis tool was found in using Maple symbolic mathematical software to try to solve some of the differential equations. Some of the solutions were given in terms of the little known "Lambert W function", W(x). For our applications, the solution to $xe^x = a$ is $x = W(a)$. The derivatives of W(x) are relatively simple functions of W(x). The Lambert W function seems to provide the solution to a number of the steps in the solution of the R-L-diode halver.

The above tools are appropriate to exponential functions. However, the depletion capacitance (4) is not exponential. After some searching, a good approximation with an exponential form was found:

$$C_{depl} \approx C_{j0}\left[1 - M(M+1)\right] + C_{j0}M(M+1)\exp\left(\frac{V}{V_j(M+1)}\right) \tag{6}$$

Thus, all the nonlinearities can be expressed in terms of exponentials and their derivatives.

Considerable effort was made to apply these mathematical techniques to the

solution of the period doubling circuit of Fig. 6, but it proved intractable.

4.3.2 Parametric Pumping

The seminal book on varactor diodes was written by Penfield and Rafuse [19] in 1962. The concept of pumping is used to explain numerous phenomena including one of interest here which is "frequency division," or "subharmonic generation." Fundamental to pumping is a time varying capacitance that arises because the capacitance varies with the applied voltage. Chapter 9 of [19] is devoted entirely to "Harmonic Dividers". The analysis is developed for both small-signal and large-signal inputs. Probably of most relevance to the FISSS is the large-signal analysis. Their work is directed to a circuit that is even simpler than that shown in Fig. 6. It consists of a series linear resistance and an abrupt junction varactor with only the depletion non-linear capacitance. No inductance is considered in their analysis. Even with this more simplified circuit, the analysis is moderately complex involving matrices of Fourier coefficients. Since this work predated the microwave halver, it is surmised that their version is difficult to implement and probably less efficient. Apparently, the addition by later workers of an inductor made a considerable difference in performance and probably for the better.

One of the authors, R. Rafuse of Lincoln Laboratory, actually visited Ottawa in March of 1992, and observed the FISSS system over a period of two days. In the end, he was as mystified as anyone else as to how the FISSS worked.

4.3.3 Monostable Multivibrator Analogy

The halver has some similarity to the monostable multivibrator. At least, the multivibrator could be configured to give a form of halving. In this multivibrator, the circuit is stable until it is hit by a sufficiently large impulse, i.e. above the threshold, at which time it switches to a second state. It reverts to its stable state after a length of time depending upon values of resistors and a feedback capacitor. If a second pulse should arrive during the second state, the discharge rate of the capacitor will not be affected and the time to revert to the stable state is also unaffected. Furthermore, if the duration of the stable state is shorter than two pulse periods, then the effect is to go to the second state for every two input pulses. In effect, a halver would result. With certain modification to the circuit parameters, it may be possible to make the circuit have more analog-like characteristics than the digital-like characteristics of the standard monostable multivibrator.

It is not clear to what use this analogy can be put in solving the FISSS. If there is sufficient similarity, at least the multivibrator can be relatively easily analyzed, and then the analysis methods applied to the FISSS. If the multivibrator were actually used in a FISSS circuit, then there would be limits on the maximum operating centre frequency.

The action described here for the monostable multivibrator is not to be confused with the use of bistable multivibrators combined with appropriate gates to form flip-flops. A single flip-flop can be configured to do a digital divide-by-two.

4.3.4 Miscellaneous Nonlinear Analysis Approaches

A variety of methods have been presented in the literature for analyzing halving operations. An early reference is the book on varactors by Penfield and Rafuse [19]. There, an entire chapter is devoted to using parametric means of halving.

In [20], certain non-linear differential equations are used that lead to period doubling. They do not tie their work to any particular real circuit, and the particular differential equation examined does not appear to be one that models the halver on the FISSS. Nonetheless, the mathematical methods look very promising. They do get solutions for the steady state performance, but resort to analog computer simulation for the transient response.

In Cunningham's book, [21], a large array of methods of analyzing nonlinear systems is provided. It includes Duffing equations for subharmonics, the non-linear van der Pol differential equations that describe certain electronic oscillators, and piece-wise linear approximations for diodes. However, in the end, these circuits did not seem directly applicable to the FISSS problem, probably because they do not consider circuits with memory.

In [22] is a tutorial on the use of Wiener-Volterra analysis of nonlinear functionals. It is a very good exposition of the subject both in theory and with real examples that are compared to experimental results. It can handle nonlinear circuits with memory. It even uses diffusion capacitance as an example. The main draw back of [22] for FISSS analysis is that it is limited to "weak" nonlinearities, which seem to be ones that can be expanded in the first few terms of a power series. It does not consider subharmonics.

4.4 SIMULATIONS AND IMPLEMENTATIONS OF THE R-L-DIODE HALVER

4.4.1 Simulations

An R-L-diode halver circuit with the parameters shown in Fig. 7 was simulated using MicroSim™ PSpice®. The symbols used in Fig. 7 are slightly modified to conform to symbols used by PSpice output. The diode used was quite ordinary and was *not* a varactor.

Many aspects of the system were studied. One example is shown in Fig. 8. It shows the drive voltage at 70 MHz. The voltage V_{L1} at the diode shows the transient build up to a waveform that eventually has a period of twice the fundamental. Also shown is this same voltage as seen through a band-pass filter (BPF) centered on 70/2 MHz. This shows that it takes about 10 cycles of the fundamental frequency for the half subharmonic to build up substantially. Simulation beyond t = 500 ns shows the half subharmonic as stabilizing to a constant amplitude.

Numerous variations of the basic circuit were simulated. These included reversing the direction of the diode, and use of symmetrical pairs of inductors and diodes. The difference in results were only in the details of where halving began, phases, etc.

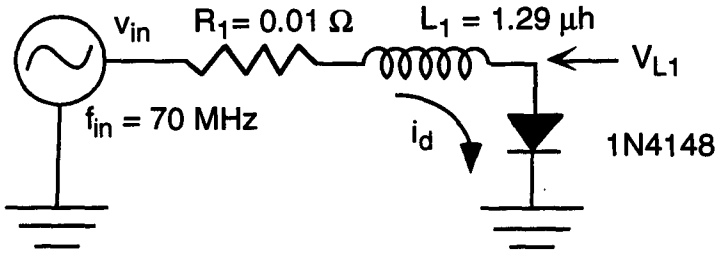

Fig. 7. R-L-diode circuit simulated with PSpice.

In an attempt to see what part of the diode contributes to the halving process, some PSpice simulations were performed with various combinations of capacitances inside the diode model shown in Fig. 4. Combinations of the depletion, diffusion, and a fixed capacitance were put in parallel with the NLR. As seen in Table 1, a rather puzzling set of results was obtained. With the diffusion capacitance alone, the circuit continued to function as a halver. Unfortunately, one of the key tests, that of using the depletion capacitance alone, could not be done because PSpice had a convergence problem.

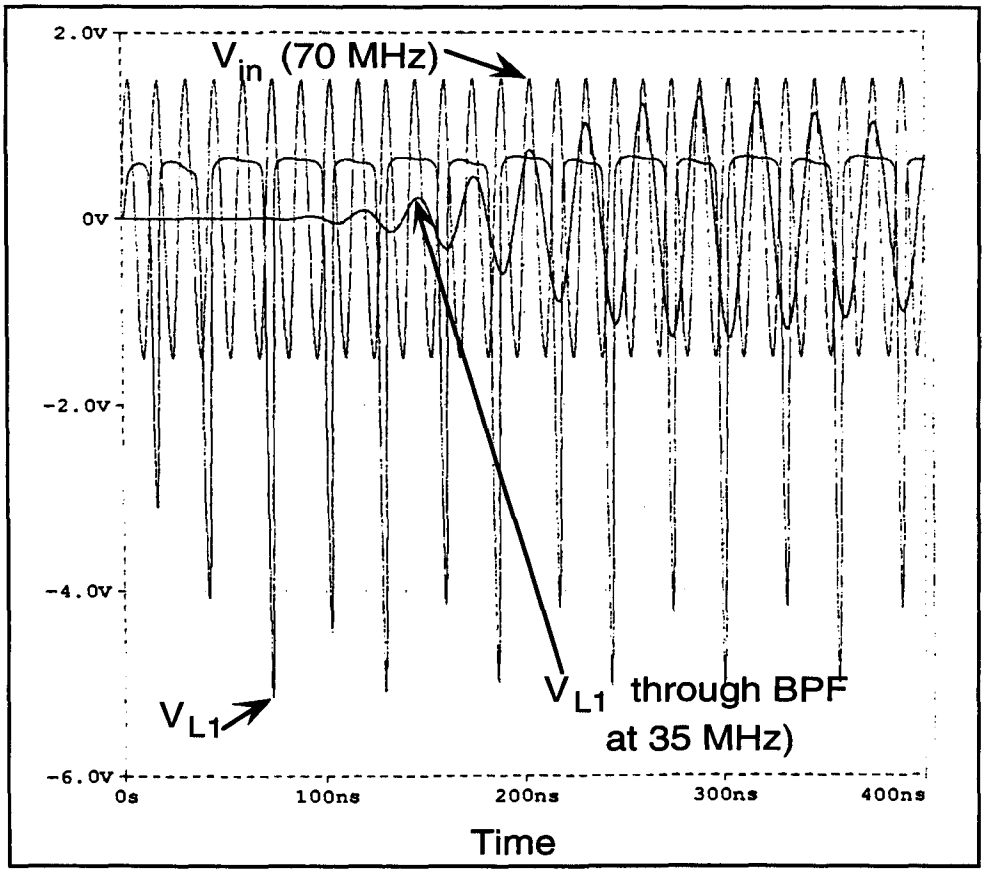

Fig. 8. A typical PSpice time output for the circuit of Fig. 7. It shows v_{in}, voltage, V_{L1}, at the diode and voltage at the diode after it has gone through a BPF centered at 70/2 MHz.

In Fig. 9 is shown the value of capacitance for three combinations of capacitors as a function of the dc voltage, V_d , applied to the junction. It was thought that this plot would give some insight as to which combination of capacitors would result in halving and which wouldn't. It was found that the region for $V_d > 0$ did not seem to be a factor but in the region $V_d < 0$, the combinations with lowest values of capacitance seemed to be the only ones that halved. The result that C_{dif} alone can result in halving is surprising because it is small in varactors, and varactors are the diodes most often used in microwave halvers! One issue to be resolved is the role of the NLR. A number of workers suggest that it is the nonlinear capacitances that lead to halving and not the NLR.

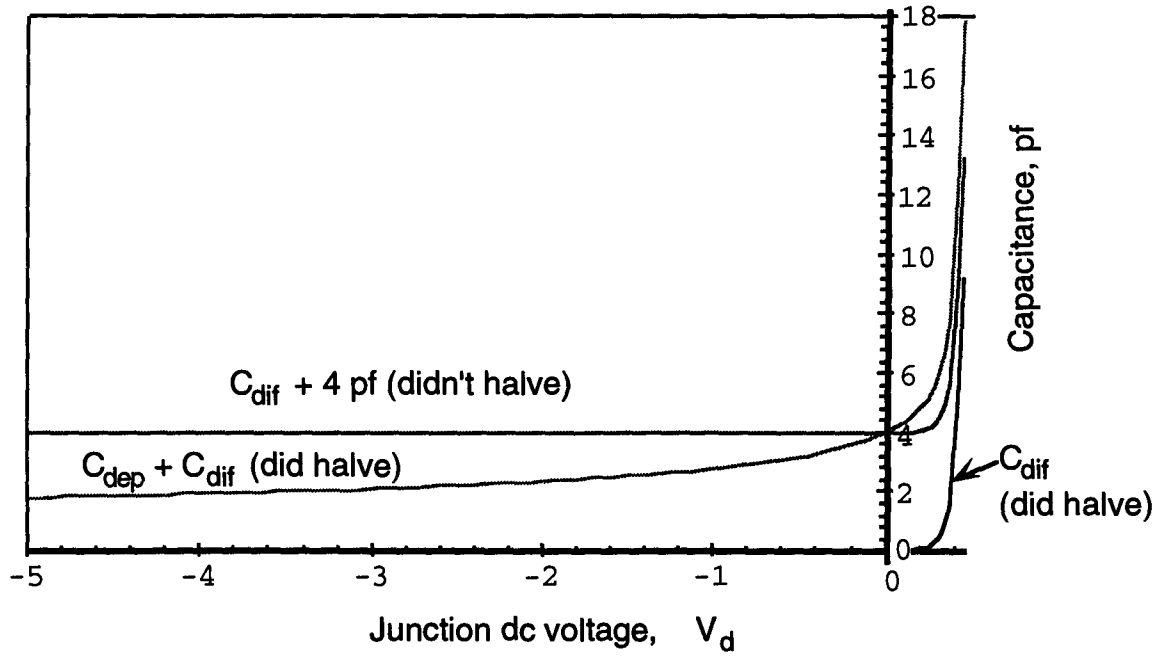

Fig. 9. Total capacitance as a function of dc junction voltage for three combinations of capacitances.

Table 1. Combinations of capacitances in the diode model and the PSpice result.

Circuit Capacitors Used	Result
C_{dif} + C_{depl} (basic halver)	Halving observed
C_{depl} alone	PSpice convergence problem, no result
C_{dif} alone	Halving observed
C_{dif} + constant external C (4 pf)	Did not halve
Constant external C (4 pf) alone	Did not halve

4.4.2 Hardware Implementation

The same circuit was also implemented in the lab. The form of the test system is shown in Fig. 10. The resistance of the frequency synthesizer combined with the 50 Ω line made the effective resistance also 50 Ω. Because of an internal DC blocking capacitor, the diode rectified the AC input at 70 MHz creating a large bias. A large inductance was added to prevent this bias offset. For a 30 dBm input signal, the spectrum as seen at "v_{probe}" is shown in Fig. 11. Unfortunately, we couldn't get results from the probe when placed right at the diode because the probe's small capacitance was as large as that of the diode, thereby upsetting the halving action. The spectrum indeed shows components at the subharmonic $f_{in}/2$ as well as at the

fractional harmonics, $3f_{in}/2$, $5f_{in}/2$, etc.

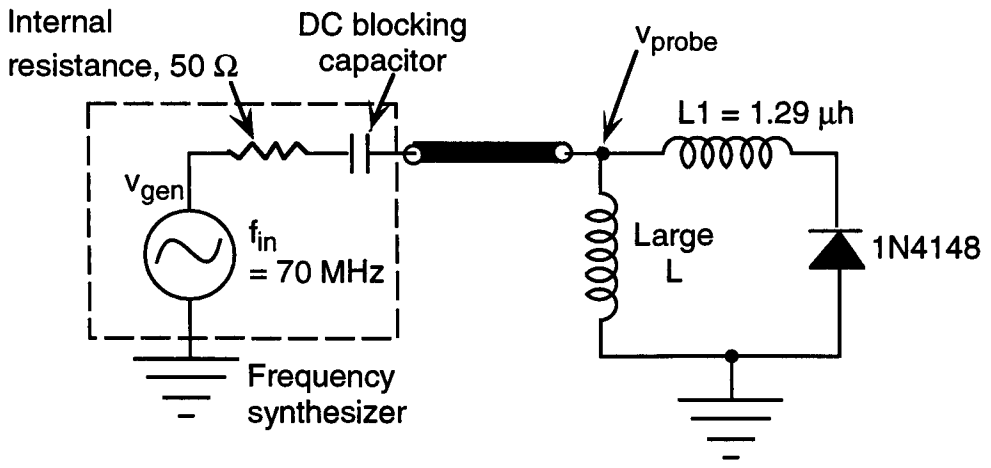

Fig. 10 R-L-diode circuit implemented in lab.

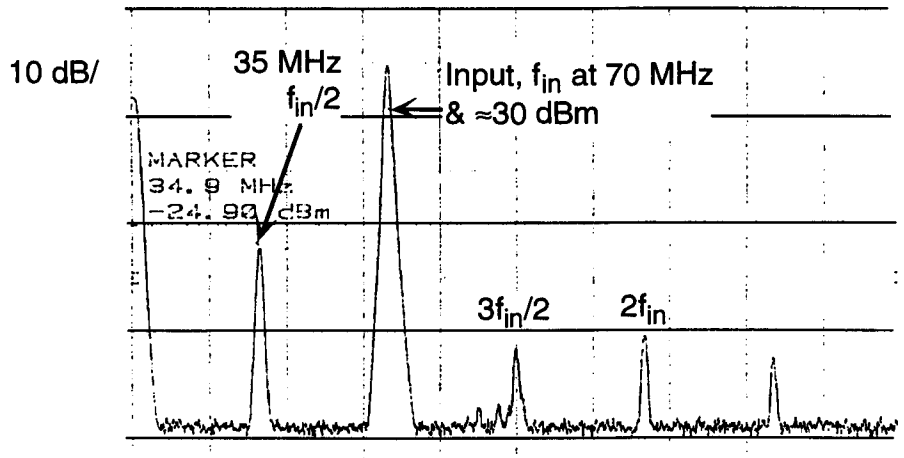

Fig. 11. Spectrum analyzer output for R-L-diode implemented in lab.

4.5 HARRISON'S ANALYSIS APPROACH FOR THE MICROWAVE HALVER

The balanced microwave halver using two varactor diodes is one of the key components of the FISSS. This halver is described and analyzed by Harrison in [24] and expanded upon (and some errors corrected) in [25]. A good overview of this form and related microwave halvers is given in [26].

From [25] and [26] an equivalent circuit is presented and is shown here in Fig. Fig. 12. The primary loop contains two varactor diodes, and is tuned to the half frequency, $f_{in}/2$ in a balanced circuit. The secondary loop taps off the half frequency

as the output into the load R_L. This output circuit is unbalanced. The objective in the halver is to convert as much power as possible into the half frequency output.

The differential equations describing the circuit was analyzed in [25] and summarized in [26]. In this analysis a number of simplifications were used. One is that the diodes are reverse biased so that the NLR (see Fig. 4) can be neglected and the diffusion capacitance is also neglected. The analysis then found steady state solutions as functions of the pump voltage, v_p, and f_{in}. The output amplitude was determined as a function of these two parameters. Of interest here are two features of the response. One feature is the sudden onset of halving action as v_p, or f_{in} reach a certain value. The second is the hysteresis of the region of halving.

Transient analysis is also performed in [25] by use of numerical analysis. The same differential equations are put into the form of a set of first-order differential equations using standard techniques. A set of four such equations is thereby generated and solved numerically for specific cases. Both the steady state and transient analyses were repeated by one of the authors. The results corroborated those in [25].

As pointed out in [26], if the circuit is forward biased, then the NLR and the diffusion equation can no longer be neglected. The analysis becomes even more complex and it appears that only numerical analysis is viable.

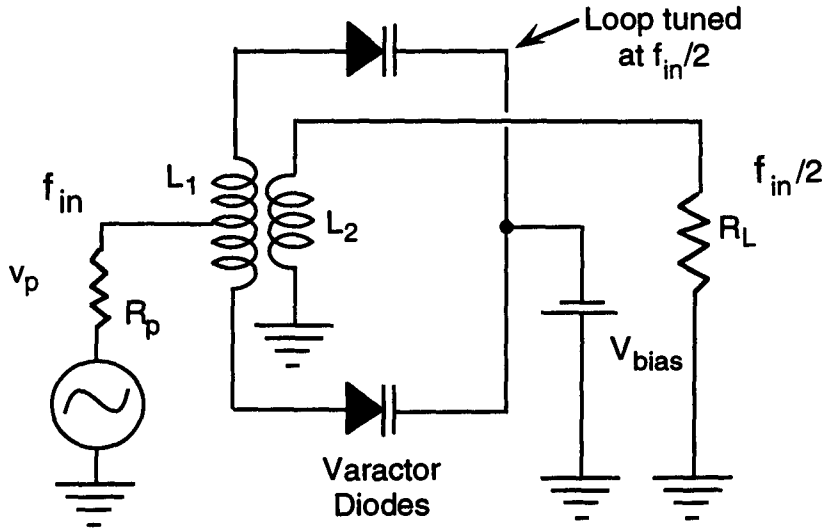

Fig. 12. Equivalent circuit for balanced microwave halver [24]- [26].

4.6 Application of Halver Analysis to the FISSS

In the above, it was found that the desired analytical solution for both the simpler R-L-diode halver, and the more complicated balanced microwave halver, when forward biased, was intractable. Only numerical analysis would yield any results. Unfortunately, numerical analysis doesn't lead to general results and would require very extensive processing. When the halver is then used in a FISSS circuit, the analysis become even more difficult for two reasons. One is that the circuit is more complex. More importantly, the halver analysis is for only a single sinewave input, whereas the FISSS must operate with multiple and possibly wideband signals. It was eventually decided that application of these mathematical attacks would be very difficult, and efforts were stopped in this direction.

It is speculated that certain aspects of the halver analysis may be usefully applied to the FISSS. In particular, it is thought that the sudden onset of halving as an input threshold is exceeded may hold a key to the explanation. At this onset, power is converted to the half-frequency band at $f_{in}/2$ thereby reducing the reflected power at the signal frequency band at f_{in}.

5. PERFORMANCE CRITERIA AND RESULTING CIRCUIT REQUIREMENTS

5.1 SUPPRESSION FACTOR VS SNIIMR

Most of the limited literature on the FISSS primarily concentrated on measuring the suppression factor. The single-tone suppression factor (*STSF*) is defined as:

$$STSF|_{dB} = P_{in}|_{dB} - P_{out}|_{dB} \tag{7}$$

where $P_{in}|_{dB}$ is the input power of a single tone in dB, and $P_{out}|_{dB}$ is the output power. This can be measured with no other signal present, or in the presence of a much smaller signal, which can be either narrow or wideband. The *STSF* is determined by measuring how much the peak of the interference power spectrum falls upon turning on the FISSS device. This measure is not very instructive and can be quite misleading. First of all, it is applicable only to single-tone interference. Secondly, it does not take account of the fact that the FISSS operation causes the appearance of intermodulation products within the operating band. Therefore, while the jamming tone is being suppressed by a large amount, this improvement is partially offset by the increase in intermodulation products.

A much better measure, used in [12] and elsewhere, is the signal-to-noise-plus-interference-and-intermodulation-products ratio, SNIIMR, measured at the output of the suppression device, i.e.

$$SNIIMR \equiv \frac{C_{out}}{N_{out} + J_{out} + IM_{out}} \tag{8}$$

where C_{out}, N_{out}, J_{out}, and IM_{out}, are signal, noise, interference, and intermodulation product powers, respectively. The IM_{out} and the *SNIIMR* will be discussed in more detail later.

5.2 PROCESSING GAIN

In Section 2.1, processing gain (PG) was defined for a variety of methods of combating interference. These methods include spread spectrum, antenna spatial discrimination, and error-correction coding. Such definitions are fraught with hidden problems that can lead to misleading conclusions. Nonetheless, we will define a PG for the FISSS, PG_{fisss}. In (1), the various methods are tied together to give a total overall PG that is the product of the individual PG's.

Because of the addition of intermodulation products when the FISSS is used, an indirect method of defining processing gain is used. The system under study is set

up using the FISSS and a jammer with total average power of $J_{fisss\ on}$. A certain BER = BER_i, is obtained. Then the FISSS and the jammer are turned off. The jamming power is then increased from zero while measuring the BER. The jamming power, $J_{fisss\ off}$, that again gives BER = BER_i, is recorded. Then

$$PG_{FISSS} = \frac{J_{fisss\,on}}{J_{fisss\,off}} \tag{9}$$

If spread spectrum is being used simultaneously, the use of this definition automatically accounts for the spread spectrum processing gain, PG_{ss}. In fact, the value of PG_{ss} need not be known for the determination of PG_{fisss}. Also, intermodulation products are automatically included in this definition.

Usually, the value of PG_{fisss} can be more easily measured than the *SNIIMR* because the *SNIIMR* is composed of numerous complicated components that aren't easily measured in aggregate. Furthermore, since PG_{fisss} is based upon BER and BER is the value that is actually desired, then measurement of PG_{fisss} by definition (9) leads to the desired BER anyway. Nonetheless, some knowledge of *SNIIMR* will be seen to give some useful insights.

6. INTERMODULATION CONSIDERATIONS

6.1 ESTIMATION OF IM PRODUCTS

6.1.1 General Discussion

In this Chapter, an attempt is made to estimate the levels of intermodulation products in the FISSS in the form of the signal-to-intermodulation-products ratio (SIMR). A method of simplifying this determination of SIMR is based upon two basic conjectures. Both conjectures are based upon a variety of observations in the lab and in the literature.

First, it is conjectured that the basic suppression mechanism arises primarily from the nonlinear capacitances in resonance with the inductive parts of the circuit. Subtraction effects are not considered here. Secondly, it is conjectured that the main source of intermodulation products is the nonlinear resistance (NLR) found in the forward-biased FISSS diodes. Therefore, the suppression level and the IM levels are decoupled so that they can be analyzed separately.

In the traditional analysis, nonlinear devices without memory are considered. By "memoryless", it is meant that the output is an instantaneous nonlinear function of the input and therefore involves no delays. In circuit terms, "memoryless" implies that there are no reactive devices such as capacitors or inductors. One example of such memoryless nonlinear devices is the NLR. Others are detectors, mixers, and TWTs.

In passing two or more signals through any memoryless nonlinearity, intermodulation products will arise. A standard measure is the intermodulation products arising from a two-tone test. In this section, an attempt is made to estimate the levels of such products arising between a small tone and a large one.

Consider a waveform consisting of two sine waves

$$w(t) = a\cos(\alpha) + b\cos(\beta) \tag{10}$$

where

$$\alpha = 2\pi f_a t + \phi_a \text{ and } \beta = 2\pi f_b t + \phi_b \tag{11}$$

The sine wave $a\cos(\alpha)$ will be assumed to represent a small desired tone and $b\cos(\beta)$ will be the large interfering tone so that $|b| >> |a|$.

In general analysis, the response is often represented as a power series

$$g(w(t)) \approx c_0 + c_1 w(t) + c_2 w^2(t) + c_3 w^3(t) + \ldots \tag{12}$$

where the coefficients $c_0, c_1 \ldots$ depend upon the nonlinearity. If terms only to the

third power in (12) are retained, there will be spectral components at dc, f_a, f_b, $2f_a$, $2f_b$, $3f_a$, $3f_b$, $f_a \pm f_b$, $2f_a \pm f_b$, and $2f_b \pm f_a$. If a band-pass filter follows this nonlinearity, and f_a and f_b are within this band, then cross product terms at frequencies $2f_a - f_b$, and $2f_b - f_a$ will also likely be in the band. These two terms are referred to as the third order intermodulation (IM) products. These third order IM products are generally the most important IM products to be considered. Fifth and higher order generally will fall outside the band-pass region. Note that a 5th power nonlinearity can generate a third order IM but was not considered in (12). The in-band terms are found to be

$$\begin{aligned} g(w(t))_{in\,band} \approx & \left(c_1 a + 3/4 c_3 a^3 + 3/2 c_3 a b^2\right)\cos(\alpha) \\ & + \left(c_1 b + 3/4 c_3 b^3 + 3/2 c_3 a^2 b\right)\cos(\beta) \\ & + 3/4 c_3 a b^2 \cos(\alpha - 2\beta) \\ & + 3/4 c_3 a^2 b \cos(2\alpha - \beta) \end{aligned} \tag{13}$$

which includes the two tones of interest plus the two third-order IM products.

For $|b| >> |a|$, the IM product at α - 2 β is much larger than the one at 2α - β, which can then be ignored. Also, if c_1 and c_3 are of the same order of magnitude, then it can be seen that the ratio of the signal component at $\cos(\alpha)$ to the main third order IM product is

$$\frac{c_1 a + 3/4 c_3 a^3 + 3/2 c_3 a b^2}{3/4 c_3 a b^2} \approx 2 \tag{14}$$

which shows the that the main third-order IM product can be about only 6 dB below the desired signal.

6.1.2 The Nonlinear Resistance (NLR)

In the previous subsection, the level of the IM product for two tones into a general power series nonlinearity was considered. Now, the IM product arising from a diode NLR will be considered. Suppose that $w(t)$ represents the voltage at the junction to a diode NLR with the I-V relationship (2). Then the resulting current has the form

$$I = I_s\left[e^{C_1(V_{dc}+w(t))} - 1\right] \tag{15}$$

where $C_1 = q / nkT$ is a constant depending upon the particular diode used, V_{dc} is the DC bias voltage, and $w(t)$ is the varying junction voltage, which for the two tones is given by (10). The Jacobi-Anger expansion (5) can then be applied. The AC part of the

exponential for two tones is then

$$\begin{aligned} e^{C_1 w(t)} &= I_0(C_1 a)I_0(C_1 b) \\ &+2I_1(C_1 a)I_1(C_1 b)\cos(\alpha)+2I_1(C_1 b)I_1(C_1 a)\cos(\beta) \\ &+2I_1(C_1 a)I_2(C_1 b)\cos(\alpha-2\beta) \\ &+2I_2(C_1 a)I_1(C_1 b)\cos(2\alpha-\beta) \end{aligned} \tag{16}$$

which parallels (13) for the power series expansion. In order to obtain some idea of the values, consider a 1N4148 diode, which was used in some the experiments. For this diode, $C_1 = 21.6$. Let the input SIR be $SIR_{in} = (a/b)^2$ and the resulting SIMR be

$$SIMR = \left(\frac{2I_1(C_1 a)I_1(C_1 b)}{2I_1(C_1 a)I_2(C_1 b)+2I_2(C_1 a)I_1(C_1 b)} \right)^2 \tag{17}$$

Then a was chosen as 0.01 V and b varied to give various values of SIR_{in}. A plot of $SIMR$ as a function of SIR_{in} is given in Fig. 13. It shows that at SIR_{in} > -10 dB, the $SIMR$ is very large. However, as SIR_{in} decreases below -10 dB, the $SIMR$ gets quite low approaching 0 dB for very small SIR_{in}. Similar results have been noted by others for limiters.

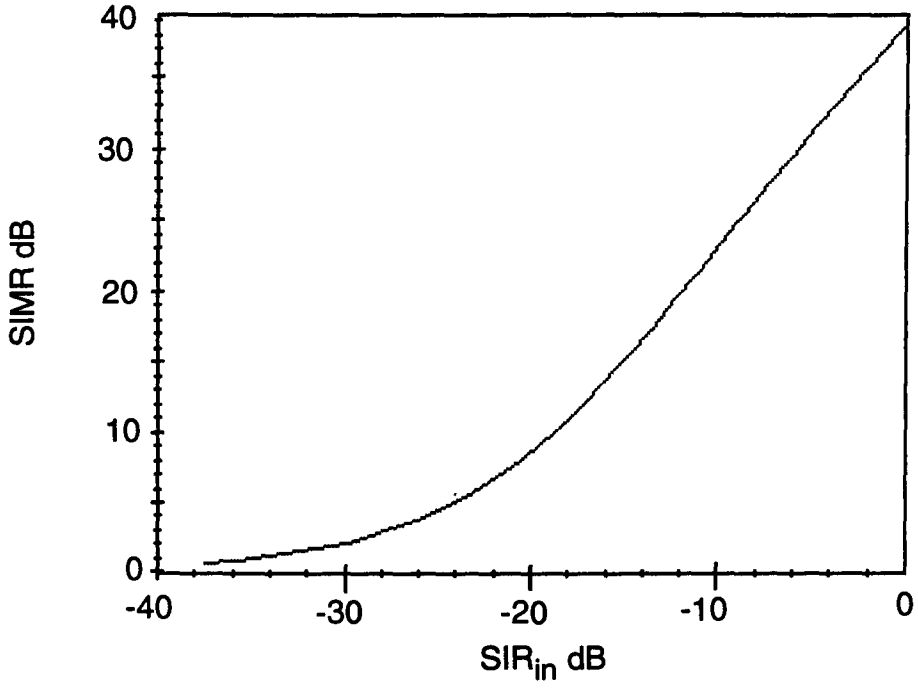

Fig. 13. A plot of $SIMR$ as a function of SIR_{in} for two tones in a 1N4148 diode.

6.1.3 Two-Tone Measurement of Third-Order IM Product

Some measurements were made on the 10-GHz FISSS devices to get some notion of the level of the resulting third-order IM products. A large interfering signal was set at the centre of the operating range and a small tone was swept across one half of the range. The IM product would then appear in the other half. Some results are shown in Fig. 14, where the small signal is swept in the lower half, and in Fig. 15, where the small signal is swept over the upper half. In Fig. 14, it is seen that over much of the range, the IM is actually larger than the signal. The reverse is true in

Fig. 15. Since the response on the upper side tends to be larger in both cases, it could be concluded that the response of the FISSS itself is unsymmetrical, and, therefore, the signal and the third-order IM product are roughly the same. This result roughly substantiates the conclusion made earlier based upon Fig. 13.

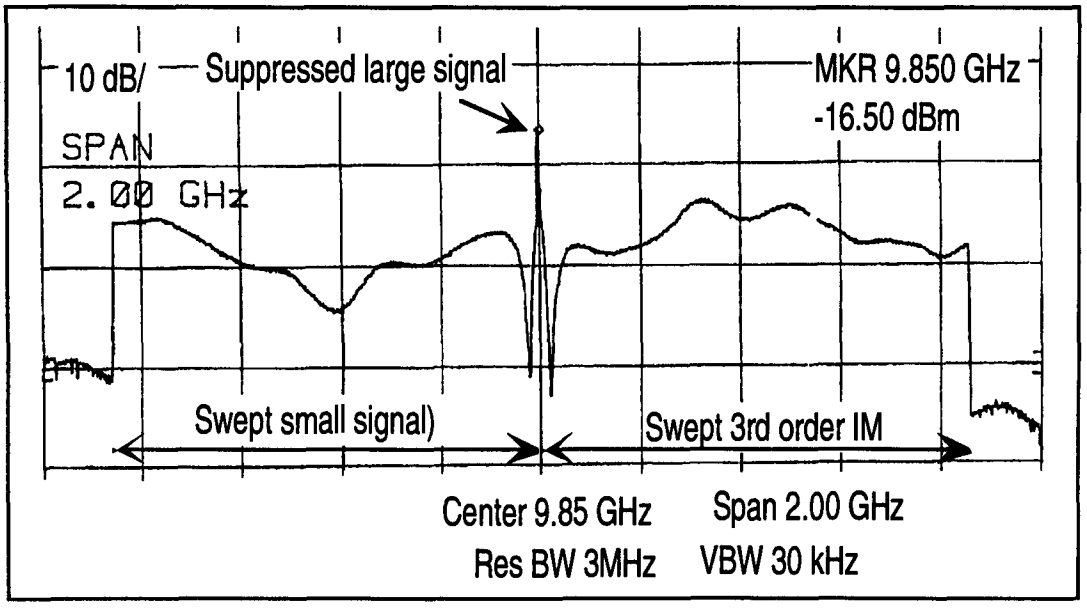

Fig. 14. The spectrum for the 10-GHz FISSS arising from a large tone centered at 9.85 GHz with a small tone swept over the lower range of 9.0 to 9.85 GHz. The third order IM product is the mirror image sweeping from 10.7 to 9.85 GHz. The input SIR = –18 dB.

6.1.4 Limiter Model

A number of people interested in the FISSS have wondered if it behaves in some manner like a limiter. In fact, most of the other nonlinear suppression devices use various forms of limiters. The broader issue has not been resolved. However, the narrower issue of IM products can probably borrow from work on interference suppression devices that use limiters. In Abrams [23], the introduction notes that

with a "strong" nonlinearity and two tones with one much larger than the other, the small tone is suppressed by about 6 dB, which is the well known small-signal-suppression effect. Also, the third-order IM product has an amplitude equal to the small signal, which agrees with the conclusion above based upon Fig. 13.

More detailed analysis of IM products through various forms of limiters used in suppression can be found in a number of places such as Jain *et al* [12], which considers variations of the dead-zone limiter, and [11] which considers methods such as the "Smart AGC".

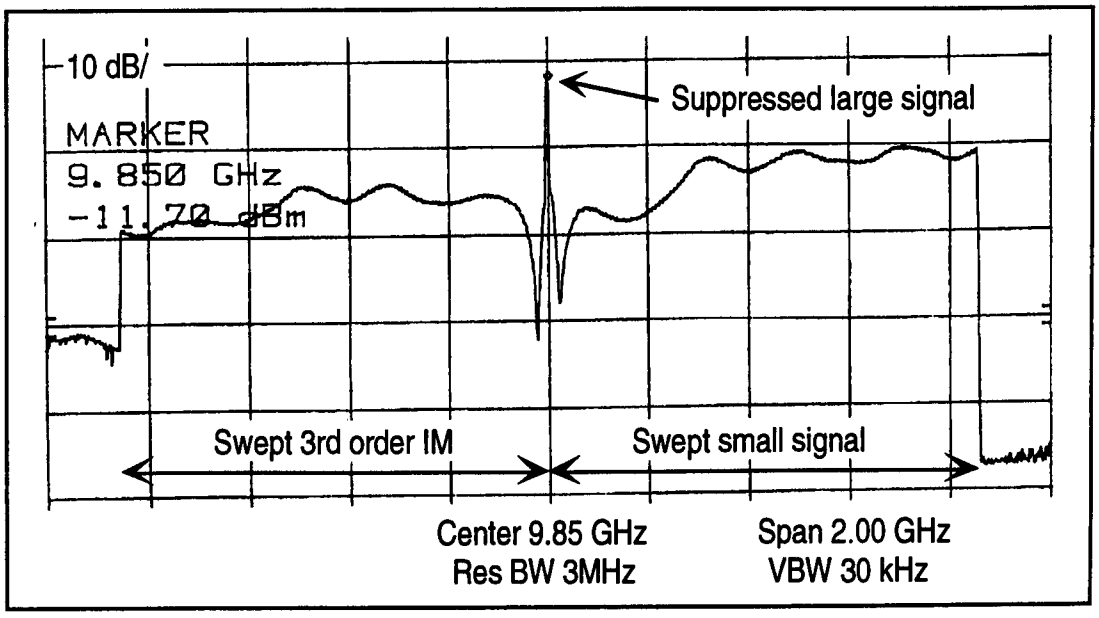

Fig. 15. The spectrum for the 10-GHz FISSS arising from a large tone centered at 9.85 GHz with a small tone swept over the upper range of 9.85 to 10.7 GHz. The third order IM product is the mirror image sweeping from 9.85 to 9.0 GHz. The input SIR = –18 dB.

6.2 Extension to Non-Zero Bandwidth Signal and Interference

Two-tone analysis and tests primarily are for estimating the third-order IM products. They don't tell us what happens when the signal and possibly the interference are of non-zero bandwidth. Even for simple nonlinearities, this analysis is very difficult. For the NLR, the analysis would be quite difficult so that here, only a guideline as to how the analysis would proceed is given.

In general, (10) and (11) become

$$w(t) = a(t)\cos(\alpha(t)) + b(t)\cos(\beta(t)) \tag{18}$$

where $\alpha(t) = 2\pi f_a t + \phi_a(t)$ and $\beta(t) = 2\pi f_b t + \phi_b(t)$ (19)

Here, $a(t)$ and $b(t)$ can be viewed as amplitude modulation of the carrier, and $\phi_a(t)$ and $\phi_b(t)$ are phase modulation of the carrier. It is assumed that the signal and interference are narrow band signals, that is, their bandwidths are small compared to their carrier frequencies, f_a and f_b, respectively. Define

$$A(f) = \mathcal{F}\left(a(t)e^{\phi_a(t)}\right) \tag{20}$$

and

$$B(f) = \mathcal{F}\left(b(t)e^{\phi_b(t)}\right) \tag{21}$$

where '$\mathcal{F}$' denotes the Fourier transform. As some hint on how the time signal and the spectrum are changed by the nonlinearity, consider the power series nonlinearity but with the two tones replaced by the narrow band version. Take only the first term in (13). It now becomes

$$\left(c_1 a(t) + 3/4 c_3 a(t)^3 + 3/2 c_3 a(t) b(t)^2\right)\cos\left(2\pi f_a t + \phi_a(t)\right) \tag{22}$$

The phase function is still intact. However, the amplitude portion now consists of the desired term plus two others that have amplitude modulations differing from that of the desired signal. The Fourier transform of (22) is

$$\begin{aligned} &1/2 c_1 A(f - f_a) + 3/8 c_3 A(f - f_a) * A(f - f_a) * A(f - f_a) \\ &+ 3/4 c_3 A(f - f_a) * B(f - f_b) * B(f - f_b) \end{aligned} \tag{23}$$

where the '*' denotes the convolution operation. Only the components at positive carrier frequencies are shown. The first term is the desired signal centered at $f = f_a$. The second term consists of the triple convolution of the desired signal, which will spread the spectrum. The third term consists of the convolution of the desired signal with the double convolution of the interfering spectrum. Such Fourier analysis can be performed for the other terms of (13) to reveal what the form of the main interference and the IM products take. Furthermore, if any of the signals are random variables such as noise or random data signals, then the spectral analysis will get even more complex with correlation functions and power spectral densities being required.

The two tones through the NLR in (16) can also be replaced by narrow band signals and similarly expanded. The spectral analysis then needed would necessitate Fourier transforms of the various modified Bessel functions, thereby increasing the difficulty of analysis.

7. SOLUTIONS TO THE INTERMODULATION PROBLEM

7.1 THE ABRAMS CANCELLATION METHOD

One clever way of getting around the IM-product problem has been introduced by Abrams [23]. The method involves modifying the transmitted waveform, and also modifying the demodulator in such a way that the effect of the third-order IM product is greatly reduced. Then, one needs only to be concerned with the reduction in the interference, which can be quite considerable. This method is waveform specific so that the modulator and demodulator have to be designed for the particular waveform.

The method applies only to phase-modulated signals such as PSK, QPSK, etc. with constant envelopes. Thus, it is only necessary to consider the phase terms in expansions such as (22); there are no induced amplitude modulations to correct. The technique uses the fact that the IM terms have factors such as $\cos(2\alpha(t)-\beta(t))$. The doubling of the phase term, $\alpha(t)$, of the signal can mean that the modulation is completely changed. Abrams [23] devised modified waveforms and demodulation circuits that take advantage of such phase changes to eliminate the effects of the third-order IM products as degradations.

7.2 EXTRA PROCESSING GAIN

It is shown in the literature that for many nonlinear suppressors, the output SNIIMR often has a fixed maximum obtainable value, usually less than 0 dB, regardless of the value of the input SNIR. This fact means that these suppressors can have very large suppression factors if the input SNIR is very small, but still result in an output SNIIMR < 0 dB. Such a value in digital communications usually leads to unacceptable BER. Therefore, all these systems need some extra boost to get the last few dB needed for acceptable BER. Obviously, spread spectrum is an obvious method. Only a small amount of spread spectrum processing gain is usually needed to obtain these few dB. Also, low-rate error-correction coding may be sufficient to supply this extra processing gain.

In the current push for ever increasing data rates, there is a problem with spread spectrum. The spread-spectrum processing gain for a given spread bandwidth, decreases inversely proportional to information bandwidth. However, it would seem possible with nonlinear interference suppressors to provide the main part of the processing gain against large jammers, and to use only minimal spread

spectrum to compensate for the effects of the IM products. It is speculated that a spread spectrum processing gain of about 6 dB would be sufficient for acceptable performance. At 6 dB processing gain, the data bandwidth could then be as large as 1/4 of the spreading bandwidth.

8. DESIGN AND MEASUREMENTS ON 1.5 GHZ FISSS

8.1 INTRODUCTION

The original FISSS built for us in industry operated at 10 GHz. It was thought that more could be learned about fundamental operation by building one in house at a lower frequency so that side issues such as parasitics become negligible. Such a FISSS was designed and built in microstrip. The circuit layout is shown in Fig. 16.It mainly consists of three circuits: the circulator, non-linear resonator and the DC bias circuit. The non-linear resonator consists of a coupled pair of equal lines each of them being reactively loaded with a varactor diode. The DC bias circuit is made of two quarter-wave sectioned transmission lines in series. This makes it behave as an open circuit to the main circuit. The DC voltage is applied at the effective short of the bias network. Here, the two DC bias circuits on the top and bottom are to provide optimal circuit balancing.

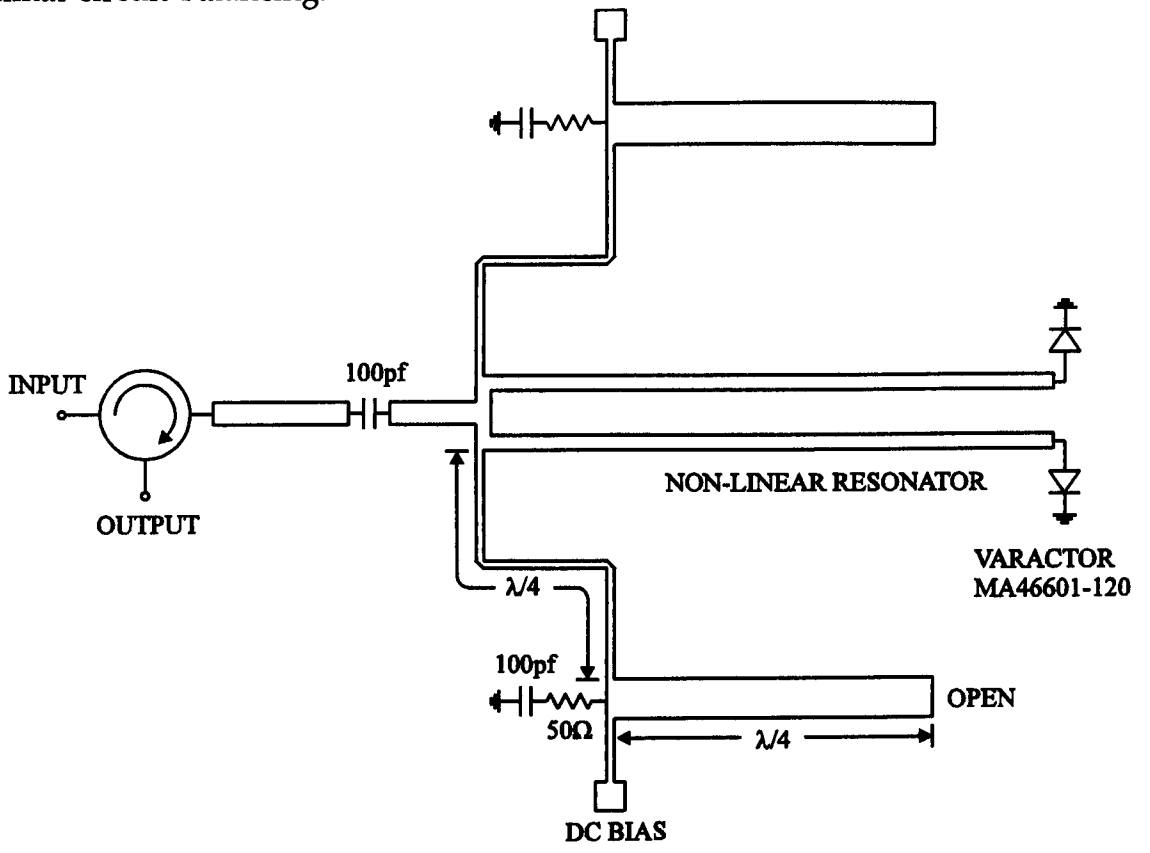

Fig. 16. The layout of the FISSS circuit operating at 1.5 GHz.

The design of the non-linear resonator is based on the varactor frequency divider described in [15]. As an initial trial, the width of the coupled-line was made arbitrarily narrow and the spacing between the lines was chosen. With the width and spacing known, the coupled-line even and odd mode characteristic impedances were calculated. The coupled-line length was then found by fixing the zero-bias resonance frequency at $f_{in}/2$. The 1.5 GHz FISSS was then assembled and tested.

The first parameter of the FISSS to be characterized is the single-tone suppression factor (*STSF*) as defined in (7) in the absence of any other signal. It is a function of at least 3 variables, namely, the input frequency f_{in}, input power level P_{in} and the DC bias voltage V_{bias}. The characteristic of the FISSS as a function of the above variables is discussed in more detail below:

8.2 STSF Versus Frequency for Fixed P_{IN} and Fixed V_{BIAS}

In Fig. 17 is shown the output power versus frequency characteristic. Here, the input power was kept constant at about 6.0 dBm as shown and the FISSS was biased at 0.4V. From these curves, the optimum STSF was found to be about 20 dB at 1.5 GHz. Furthermore, the bandwidth of the FISSS can be found. Chaotic behaviour was also found at certain frequencies.

8.3 STSF Versus P_{IN} for Fixed Frequency and Fixed V_{BIAS}

Fig. 18 shows the single tone suppression factor versus the input power level at 1.5 GHz and the bias voltage at 0.4V. Again, the maximum *STSF* was about 20 dB near 6.0 dBm input power level. As the input power level was increased further, the *STSF* decreased. Then it went into a short chaotic region as shown. It is seen that the performance is very sensitive to the input power level.

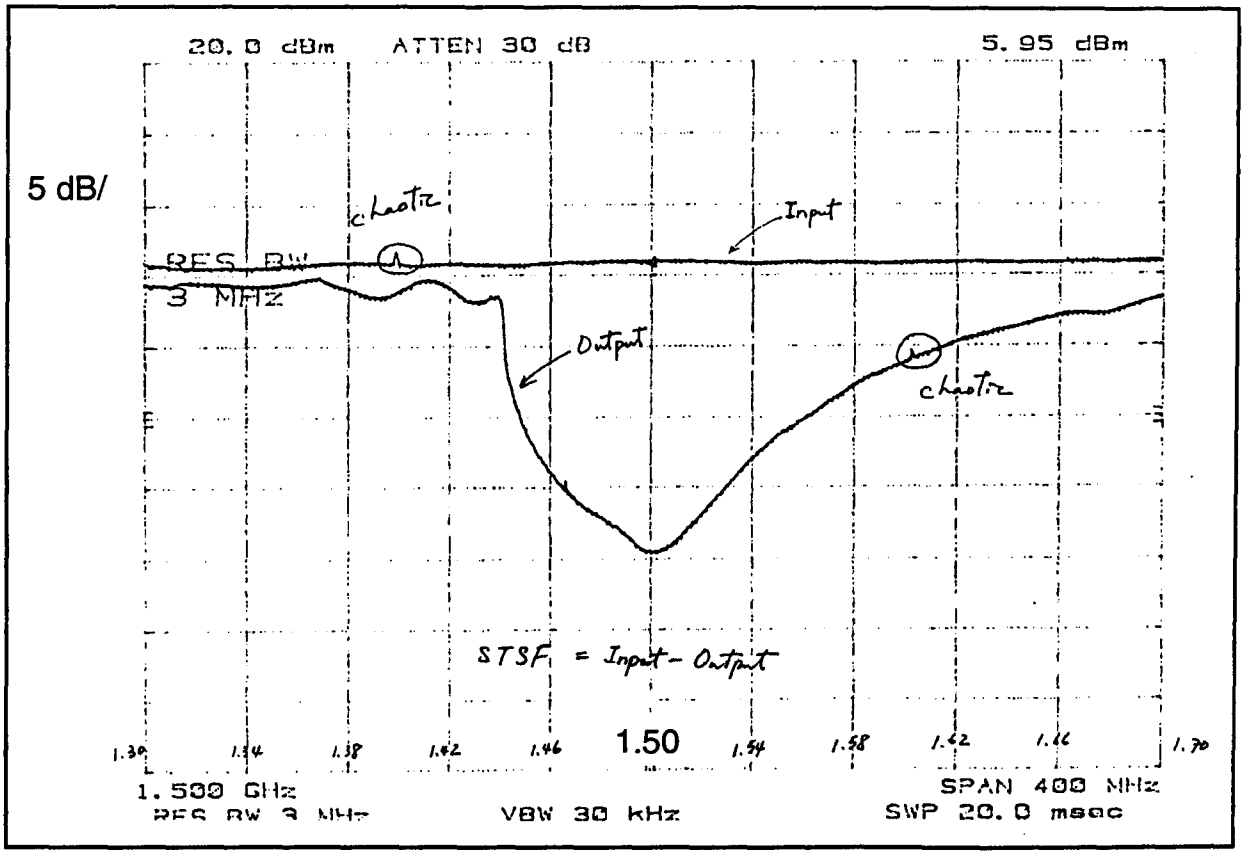

Fig. 17. Spectrum analyzer measurement of the 1.5 GHz FISSS for a single tone in. The upper line shows the input power and the bottom, the output power from the FISSS.

8.4 STSF VERSUS V_{BIAS} FOR FIXED FREQUENCY AND FIXED P_{IN}

Shown in Fig. 19 is the single-tone suppression factor versus the bias voltage with an input power level of 7.8 dBm at 1.5 GHz. It can be seen that the STSF is very sensitive to the applied DC bias voltage.

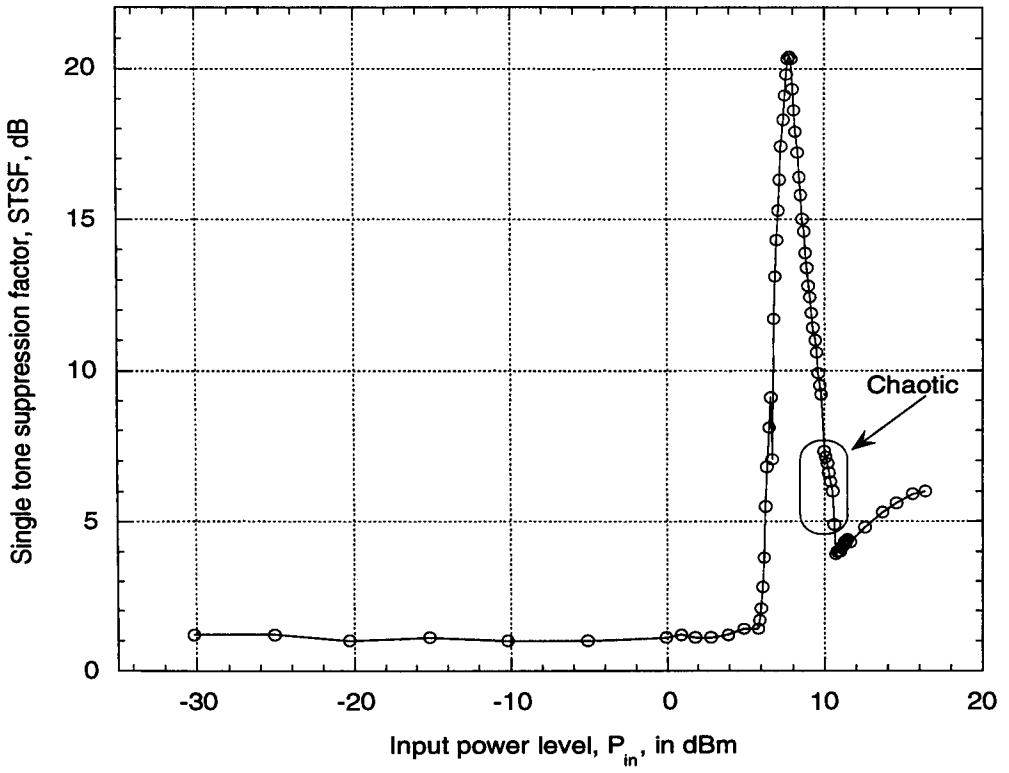

Fig. 18. A plot of STSF as a function of input power for a single tone exactly at 1.5 GHz.

8.5 SUB-HARMONICS AND INTERMODULATION PRODUCTS AT FISSS OUTPUT

In a further single-tone test, the spectrum was measured over a range wide enough to detect subharmonics with the FISSS on and off, and is shown in Fig. 20. The centre is at 1.5 GHz and bias was set for maximum suppression. The original traces were in two different colors. With the FISSS turned off, only the large peak was showing. With the FISSS turned on, this main peak dropped about 20 dB but sub-harmonic spectral components at $f_{in}/2$ = 750 MHz and $3f_{in}/2$ appeared. However, these subharmonic components are low and verifies the theory that the subharmonic and its odd multiples are cancelled because of the balanced configuration found in the circuit of Fig. 16. Because of this cancellation, no matched load was necessary for the 1.5 GHz FISSS hence reducing the circuit cost and complexity.

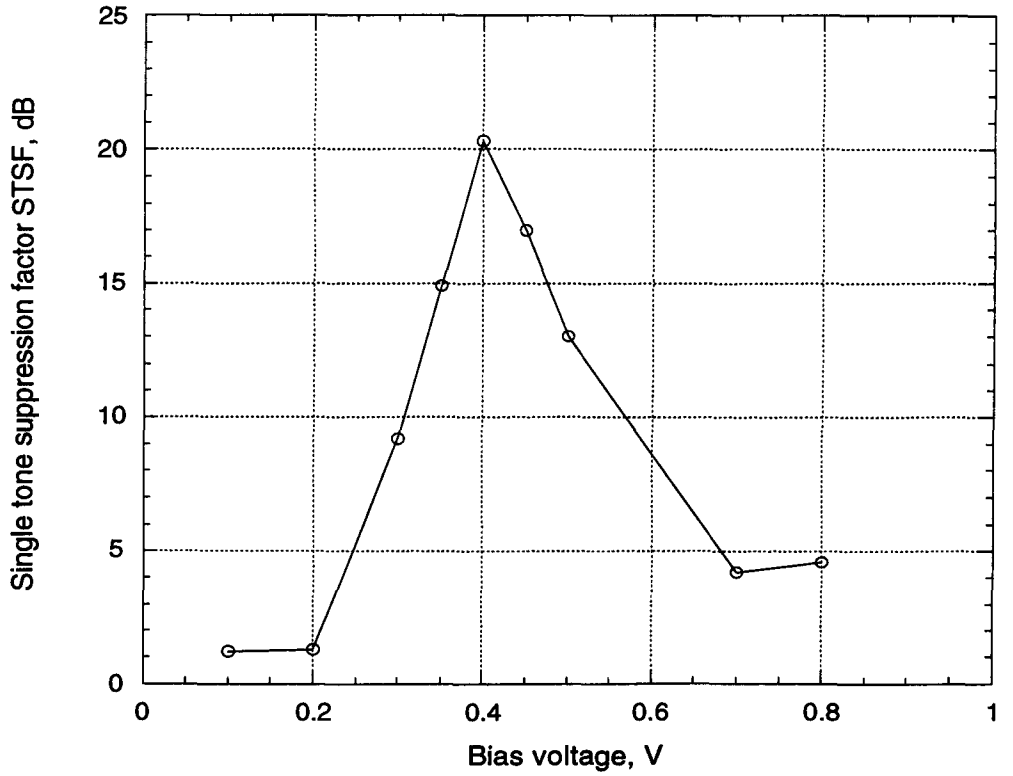

Fig. 19. A plot of STSF as a function of bias voltage for a single tone exactly at 1.5 GHz and input power fixed at 7.8 dBm.

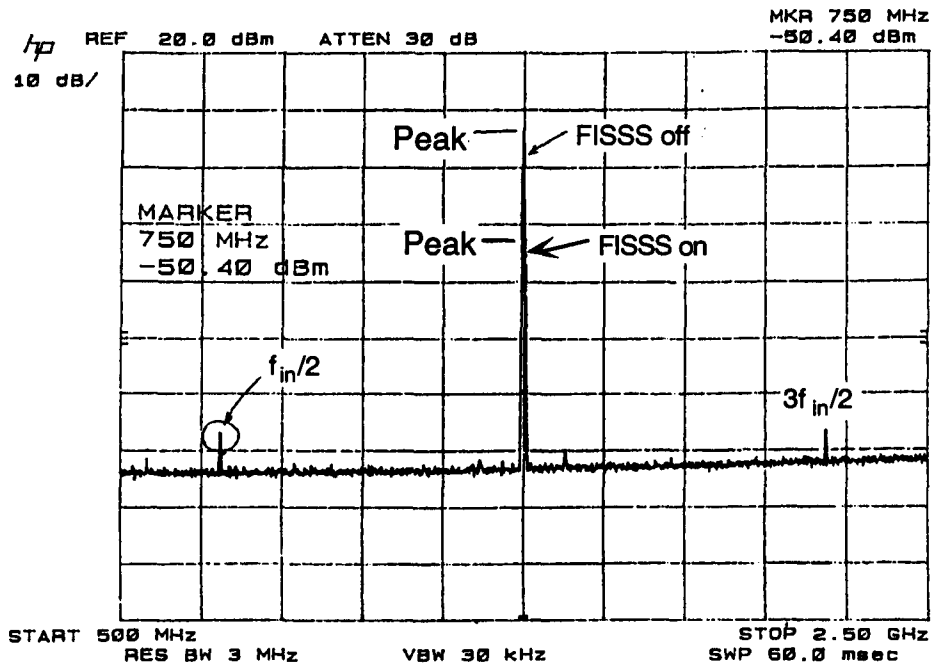

Fig. 20. Spectrum analyzer traces for the FISSS off and on, with both the bias and f_{in} (1.5 GHz) chosen for maximum suppression.

Although the balanced configuration led to reduction of components at the output at $f_{in}/2$, $3f_{in}/2$, ..., there were, unfortunately, no signs of intermodulation cancellation observed in the lab under two-tone tests. Furthermore, it was found that the suppression factor greatly degraded to only about 5 dB for the reasons not yet understood. It was concluded that that 1.5-GHz FISSS was not adequate as an interference suppressor. It was also realized that even the single-tone suppression factor of only 20 dB was too low. It is believed that by increasing the coupled-line width and improving the impedance match between the input and the non-linear resonator following the techniques of [15] would lead to more impressive suppression for both single- and two-tone tests. It would seem that it should be possible to achieve or exceed the performance of the 10 GHz FISSS described in the next section.

8.6 Some Subtraction Related Experiments

As discussed earlier, it was thought that there may be some additional reduction of the interfering signal arising from subtraction effects between the reflected and feed-through versions of the interfering signal. See Fig. 5 and the associated discussion. Some effort was made to determine and quantify these subtraction effects. The 1.5 GHz FISSS was used in this work because it was somewhat simpler to perform the necessary measurements. Much effort went into these measurements. The phase of the reflected signal was varied by using various lengths of coaxial cable. In the end it was realized that these measurements would require more effort than were actually spent for two reasons. One was that the leakage and reflected signals were very small compared to the interference. The second was that it is very difficult to distinguish signals due to circulator leakage and those reflected by the nonlinearity.

The results were inconclusive. It still appears that subtraction is an important part of the operation.

9. PERFORMANCE OF DIRECT SEQUENCE SPREAD SPECTRUM WITH 10 GHZ FISSS

In view of the lack of success with the 1.5 GHz FISSS, it was decided to perform further performance measurements with the 10 GHz FISSS built earlier in industry. It was decided to repeat much earlier tests that used direct sequence (DS) spread spectrum to provide the extra processing needed to complement the FISSS suppression.

9.1 10-GHz Test System

The approximate form of the main circuit is shown in Fig. 21. The actual centre frequency was found to be 9.7 GHz. It was noticed that the supposed connection to the "matched load" was through a thin line, i.e. a high impedance line, and was attached to the DC bias connection. Therefore, it became apparent that the output was not properly connected to a matched load, and, as found by lab measurements, the circuit operated the same regardless of the termination used at the location reserved for the matched load. Nonetheless, the half frequency, $f_{in}/2$, should still be cancelled out in the same manner as described for the 1.5 GHz circuit.

A fault of the 10-GHz microstrip is that the biasing is not done symmetrically. A more serious problem with this version of the FISSS relates to the biasing circuit itself. It was incorporated on the backside of the microstrip and had an internal temperature compensation circuit. The result was that the diodes were forward biased at fixed value of about 0.7 V regardless of the input value from the DC source. Thus, a very important parameter was not adjustable and limited the performance.

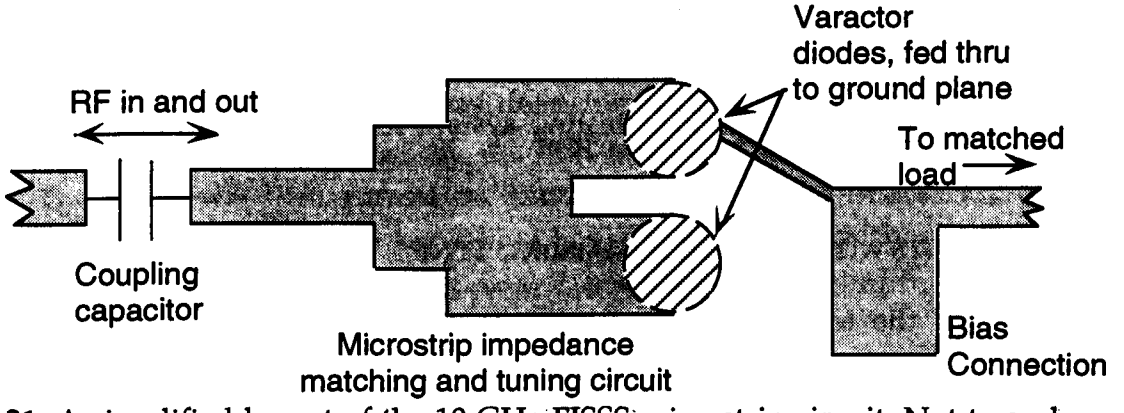

Fig. 21. A simplified layout of the 10 GHz FISSS microstrip circuit. Not to scale.

The test system is shown in Fig. 22. Data bits are generated and errors detected and counted by a Fireberd MC6000. A Loral EB 200 modem board was used to perform spreading, BPSK modulation at 70 MHz, despreading and demodulation. The 70 MHz IF was up-converted to 9.7 GHz for processing in the FISSS and then down-converted back to a 70 MHz IF. Data was generated at 1.544 Mb/s and then spread at 30.88 Mchip/s for a processing gain of 20 (13 dB). In most measurements, the jamming was a CW tone set at a power level of +13.3 dBm, which corresponded to the best suppression performance for the fixed bias to which this FISSS circuit was restricted. Considerable filtering is used. However, we could not always get the best-suited filter bandwidths or centre frequencies.

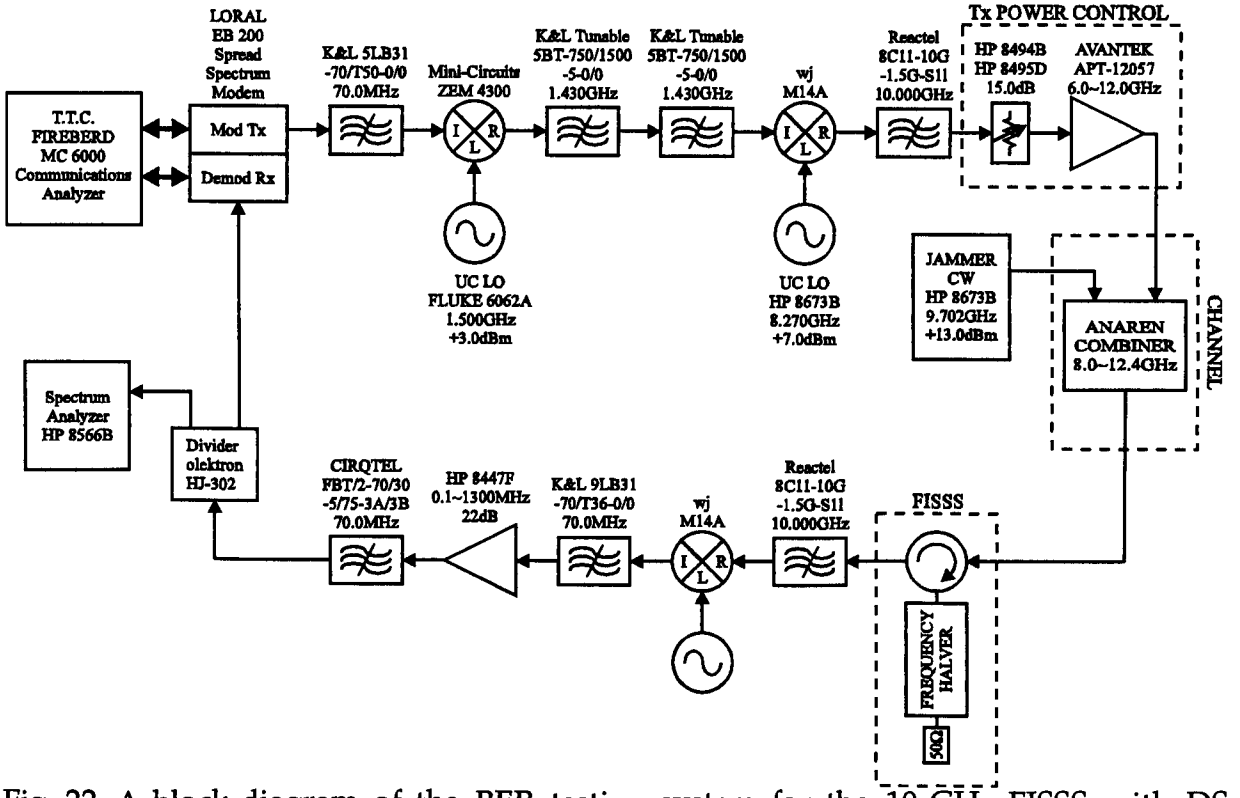

Fig. 22. A block diagram of the BER testing system for the 10 GHz FISSS with DS spread spectrum.

9.2 MEASUREMENTS WITH SINGLE CW JAMMING TONE

To illustrate the form of spectrums involved, the spectrums of the processed signal after down converting to the 70-MHz IF are shown in Fig. 23. Both the spectrum with the FISSS turned off and when it is turned on is shown. The 13.3-dBm CW interference was offset from the 70-MHz centre frequency by Δf = 2 MHz.

The jammer is seen to drop by about 20 dB. The desired signal appears to be affected by the addition of intermodulation effects only slightly since the broadband spectrum of the signal is changed only slightly. However, this observation is misleading since the intermodulation main interference product will have the form of the CW jammer convolved with the DS spread signal's spectrum. Thus, the intermodulation waveform is also wideband and is not easily distinguishable from the spectrum of the desired spread signal.

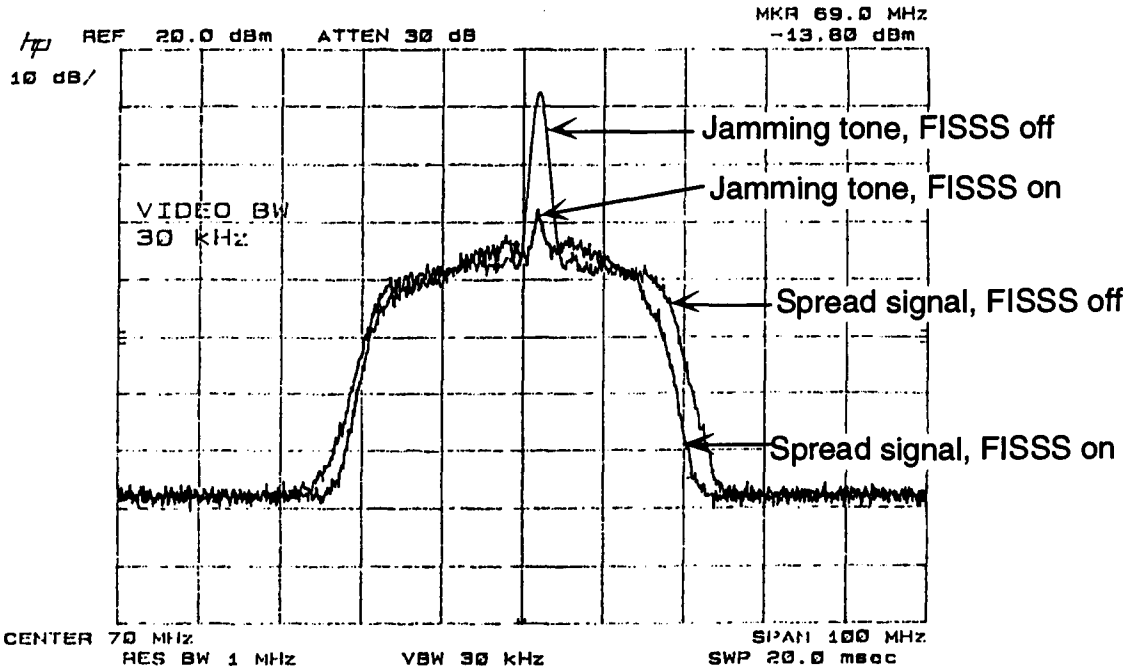

Fig. 23. Output spectrum measured at IF for a CW jammer offset by Δf = 2 MHz from the centre of the DS spread signal, for both the FISSS off and on.

The DS spread system in Fig. 22 in the absence of any jamming gave a BER of about 10^{-8} as limited by internal noise, implementation loss, etc. A series of BER measurements were then made with a single CW jamming tone at the standard setting. The first measurement was done for various offset frequencies, Δf, of the jammer. With the FISSS turned off, the BER is 0.5 and the modem completely loses sync. The FISSS was then turned on and the results are plotted in Fig. 24. At low values of Δf, the BER is high but still is better than the 0.5 without the FISSS. For offsets > 400 kHz, all values of BER were $<10^{-4}$, a very useful improvement over the 0.5 without the FISSS.

In another set of measurements, both the suppression factor and the processing gain, as defined by (9), were measured for the single-tone jammer at a number of offset frequencies. The power of the signal was C = –5.12 dBm and the power of the

jammer was at J = +7.45 dBm for a C/J of –12.57 dB. In Table 2 are summarized some typical results. It is seen that the processing gain is fairly constant over the range of offset frequencies. Also, it is somewhat lower than the suppression factor as expected. Nonetheless, the PG_{fisss} of at least 10.5 dB can be viewed as quite useful.

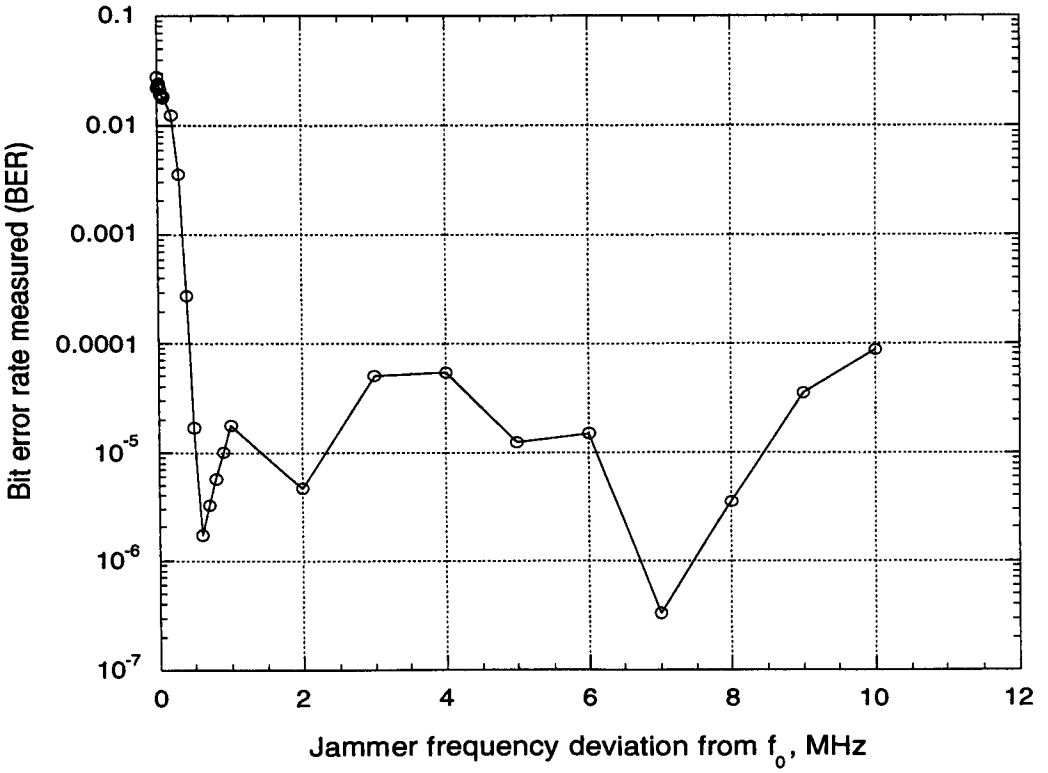

Fig. 24. Measured value of BER as a function of offset frequency of a single-tone jammer against a DS spread signal at a centre frequency of 9.7 GHz.

Table 2. Some example values of measured suppression factor and PG_{fisss}, for selected values of single-tone jammer offset frequency, Δf.

Δf, MHz	BER_i	Suppression Factor, dB	PG_{fisss}, dB
0.0	$2.2 \bullet 10^{-2}$	21.7	13.0
0.05	$2.2 \bullet 10^{-2}$	23.6	12.5
0.1	$1.8 \bullet 10^{-2}$	24.7	12.5
0.5	$1.7 \bullet 10^{-5}$	24.9	12.5
1.0	$1.8 \bullet 10^{-5}$	25.1	12.5
5.0	$1.2 \bullet 10^{-5}$	23.4	10.5
10.0	$8.7 \bullet 10^{-5}$	23.8	10.5

9.3 MEASUREMENTS WITH FM AND AM JAMMING TONES

A number of measurements were made with a sine-wave modulation superimposed on the jamming tone. Both FM and AM were tried. The jamming carrier power, J, and the desired signal power, C, were the same as in the CW jamming measurements. The spectrums for one set of FM parameters are shown in Fig. 25. The spectrum of the FM modulation is clearly shown for the trace with the FISSS off, and conforms to the spectrum predicted from FM theory. With the FISSS turned on, the FM interference appears to disappear but the overall background spectrum appears to drop. The BER was measured with the FISSS on at about $4 \bullet 10^{-4}$, which is close to the value obtained with a single-tone jammer with no FM modulation. Note that in the time domain, the FM modulated jammer has a constant envelope. Therefore, it was concluded that the FISSS can operate with wide band interference just as well as for narrow band *provided that the envelope is constant*.

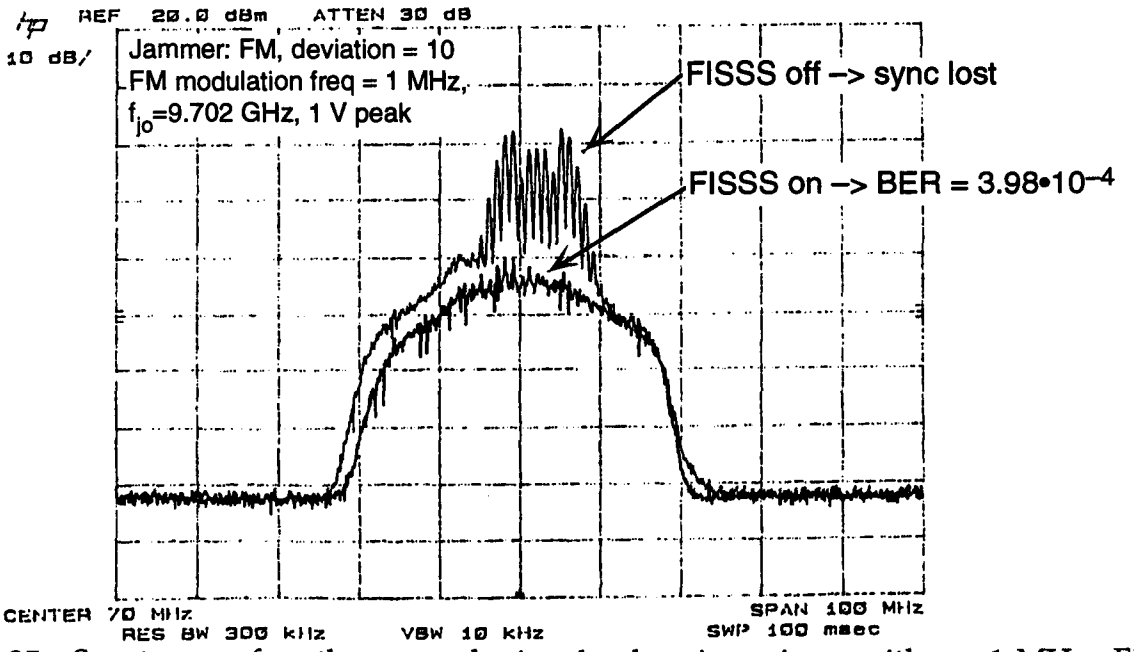

Fig. 25. Spectrums for the spread signal plus jamming with a 1-MHz FM modulation.

Finally, measurements were made with AM modulation. In most of the measurements, the system failed to achieve synchronization so that the FISSS was considered incapable of proper suppression. The reason it did not work is related to the fact that the envelope is varying and therefore, the signal is only occasionally at

the correct envelope power for maximum suppression. What is needed is some means of measuring the envelope power and using this information in a feedback loop to vary the diode bias levels.

9.4 MEASUREMENTS WITH NOISE JAMMING

A number of measurements were made with additive white Gaussian noise (AWGN) jamming over various fractions of the spread band. Examples of the effect on the spectrum are shown in Fig. 26 through Fig. 28, which are for partial-band noise jamming over bandwidths of 2.0, 4.5, and 21 MHz, respectively. These spectrums were obtained after down conversion, i.e. at 70 MHz. The suppression factor appears to be about 20 dB for the 2.0 MHz, and decreases as the bandwidth increases. The effective processing gain, as defined in (9), was measured for a variety of bandwidths and the results summarized in Table 3. Over most of the values, a PG_{fisss} of about 10 dB is achieved. When the full spread band of about 40 MHz is jammed, the PG_{fisss} falls to about 6 dB which is still useful.

Table 3. Some example values of measured PG_{fisss}, for selected values of bandwidth for partial-band noise jamming.

Noise bandwidth, MHz (%)	BER_o	PG_{fisss}, dB
2 (5%)	$4.3 \cdot 10^{-4}$	10
4.5 (11%)	$3.6 \cdot 10^{-5}$	12
21 (52%)	$2.2 \cdot 10^{-2}$	9
40 (100%)	$2.2 \cdot 10^{-2}$	6

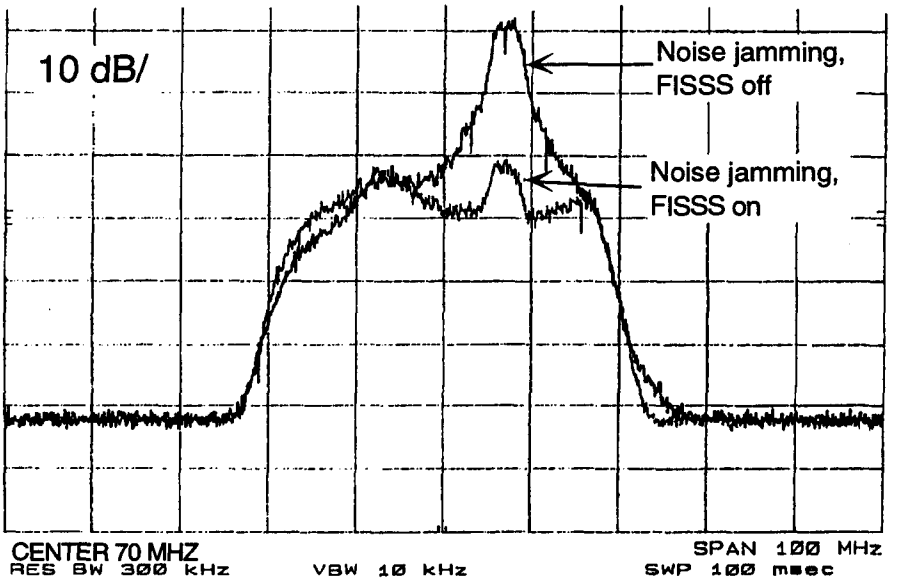

Fig. 26. Spectrums for the spread signal plus partial-band noise jamming with a 2.0 MHz width.

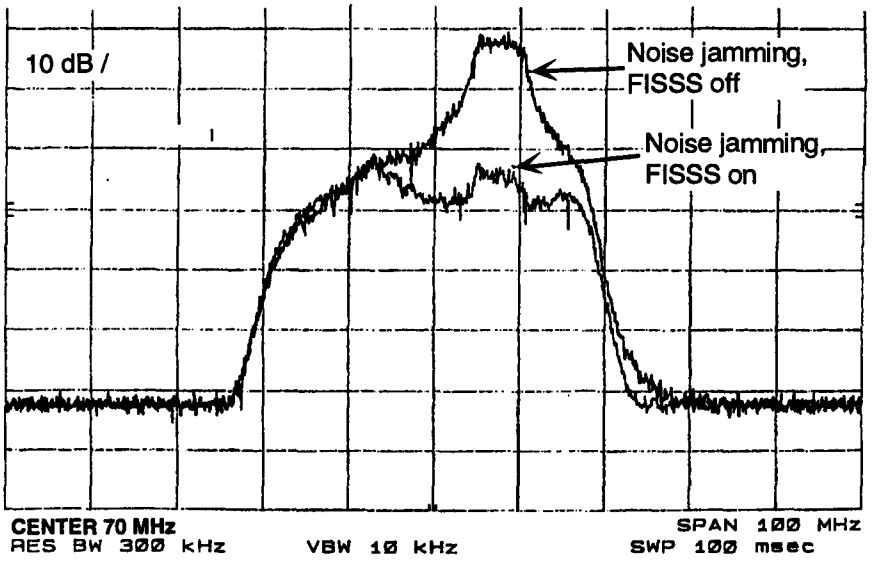

Fig. 27. Spectrums for the spread signal plus partial-band noise jamming with a 4.5 MHz width.

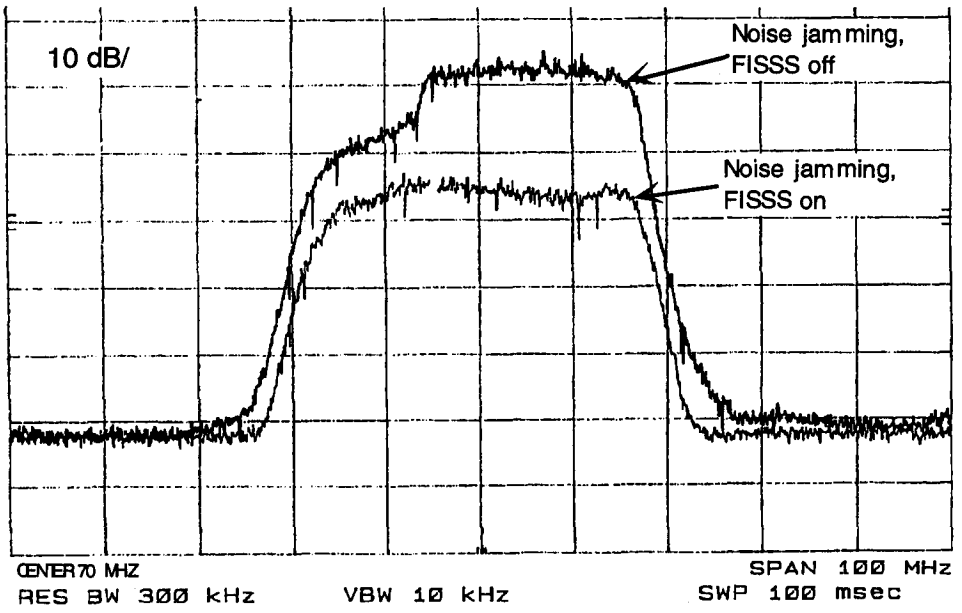

Fig. 28. Spectrums for the spread signal plus partial-band noise jamming with a 21-MHz width.

9.4.1 Heuristic Explanation of Noise Suppression

The fact that the FISSS suppresses noise interference at all was of great interest. No analysis was able to explain it, so only a heuristic argument can be given now. First note that $W_n << f_c$, where W_n is the noise bandwidth, and f_c is the centre frequency. Therefore, the amplitude of the noise has a time constant of the order of $1/W_n$, which is much larger than the period of the carrier. Therefore, it is argued that the noise amplitude holds at a particular value for a period that is long compared to the period of the carrier. Since it temporarily appears like a CW signal, FISSS action has time to come into play. If the amplitude is below the optimum for the FISSS, the output will also be small. If it is near the optimum level for the FISSS, the noise will be suppressed considerably. If it is greater than the optimum, then the noise may be suppressed only slightly. On average, the output noise will be lower. This heuristic argument does not account for the fact that the FISSS requires a certain turn on time at the given amplitude level.

10. CONCLUSION

In this work on the FISSS, advances have been made in analysis, and exhaustive experimental work has been performed.

On the analysis side, the relationships to microwave halving have been investigated at length. A number of mathematical techniques have been provided that have potential for complete analysis of the FISSS. Mathematical expressions have been developed to describe the intermodulation products. It was shown that the FISSS can suppress very large interference but there are always residual intermodulation products. As a result, a practical system must also have other processing gain of the order of 6 dB. Such modest additional processing gain can be obtained from spread spectrum or low-rate error-correction coding.

On the experimental side, some devices were designed and built to operate at 1.5 GHz. Extensive measurements were made on the basic parameters of these 1.5 GHz devices as well as on some 10-GHz devices built in industry. The FISSS, augmented by direct-sequence spread spectrum, has been shown experimentally to provide good processing gain of 10 to 13 dB against single CW tones and frequency modulated tones. More modest processing gain is achieved against partial-band noise interference. For instance, the interference suppression for the particular FISSS varied from about 10 dB for relatively narrow-band noise interference to about 6 dB for full-band interference.

There are many areas of interest for future work on the FISSS. The following research suggestions result directly from the work presented in this report:

- build a new FISSS at 1.5 GHz with better matching and resonant lines,
- develop a more accurate theory,
- try a FISSS with frequency-hopping spread spectrum,
- continue the investigation of subtraction effects,
- develop feedback methods to compensate for envelope variation,
- implement a FISSS using lumped elements,
- develop further the techniques to overcome the IM-products problem, and
- find an operational radio system with which to test and demonstrate the FISSS.

11. REFERENCES

[1] A. Gagnon, P.M. Gale, E.B. Felstead, and J.S. Wight, "Frequency–independent suppression of interference signals on spread–spectrum communications", in Conf. Record of IEEE Milcom 91, pp. 380-384, McLean VA, Nov. 5-7, 1991.

[2] A. Gagnon, "Simple circuit instantly cuts jammer signals," Microwaves and RF, pp. 135–140, 1990.

[3] André Gagnon, "Frequency independent strong signal suppressor," United States Patent Number 5,307,514, April 26, 1994.

[4] Stephen Bafia, J. Wight, and André Gagnon, "Investigation of the Frequency Independent Strong Signal Suppressor (FISSS) for Application in EHF Satcom," Final Report, CAL Corp. SSC contract no. 0135V.W8477-2-TB02, 30 Dec. 93.

[5] D. Sychaleun, E. Barry Felstead, and G.A. Morin, "Progress on the frequency independent strong signal suppressor," in Proc. IEEE Milcom 97, pp. 69-73, Monterey, CA, 3-5 Nov. 1997.

[6] E.B. Felstead and D.S. Arnstein, "Auxiliary Interference Suppression Techniques," half-day tutorial presented at IEEE Milcom '94, Fort Monmouth, October 1994.

[7] L.B. Milstein, "Interference rejection techniques in spread spectrum communications," Proc. IEEE, vol. 76, pp. 657-671, June 1988.

[8] R. Vijayan, and H.V. Poor, Nonlinear techniques for interference suppression in spread–spectrum systems," IEEE Trans. Comm. vol. 38, pp. 1060-1065, July, 1990.

[9] T. Kasparis, M. Georgiopoulos, and E. Payne, "Non–linear filtering techniques for narrow–band interference rejection in direct sequence spread–spectrum systems," in Conf. Rec. of IEEE Milcom 91, pp. 360-364, Washington, Nov. 1991.

[10] F. Amoroso & J.L. Bricker, "Performance of the adaptive A/D converter in combined CW and Gaussian interference," IEEE Trans. Comm., vol. COM-34, pp. 209-213, March 1986.

[11] Don Arnstein, Cameron Pike, and George Estep, "On–board AJ enhancement using adaptive nonlinear processing: practical aspects of smart AGC," in Conf. Record IEEE MILCOM 92, pp. 199-205, Oct. 1992.

[12] P.C. Jain, N.M. Blachman, and Paul M. Chapell, "Interference suppression by biased nonlinearities," IEEE Trans. Inf. Th., vol. 41, pp. 496-507, March 1995.

[13] J.H. Higbie, "Adaptive nonlinear suppression of interference," in Conf. Record of IEEE Milcom 88, pp. 381-389, October 1988.

[14] N.M. Blachman, "Optimum memoryless bandpass nonlinearities," IEE Proc.–I, vol. 140, No. 6, pp. 436-444, Dec. 1993.

[15] G.A. Kalivas and R.G. Harrison, "A new slotline-microstrip frequency halver," in IEEE MTT-S Digest, pp. 683-686, 1985.

[16] D. S. Arnstein, "Smart AGC: A new anti-jam device for military satellite systems," IEEE MILCOM 91, Conference Record, pp. 672-677, McLean, Virginia, Nov. 4-7 1991.

[17] P.W. Baier, and K.–J. Friederichs, "A nonlinear device to suppress strong interfering signals with arbitrary angle modulation in spread-spectrum receivers," IEEE Trans. Comm., Corres., vol. COM-33, pp. 300-302, March 1985.

[18] Martin J. Hasler, "Electrical circuits with chaotic behavior," Special Issue on *Chaotic Systems*, Proc. IEEE, vol. 75, pp. 1009-1021. August 1987.
[19] P. Penfield Jr., and R. P. Rafuse, *Varactor Applications*, M.I.T. Press, Cambridge MA, 1962.
[20] C. Hayashi, Y. Nishikawa, and M. Abe, "Subharmonic oscillations of order one half," IRE Trans. Circuit Theory, vol. CT-7, pp. 102-111, June 1960.
[21] W.J. Cunningham, *Introduction to Nonlinear Analysis*, New York, McGraw-Hill, 1958.
[22] J.J. Bussgang, L. Ehrman, and J.W. Graham, "Analysis of nonlinear systems with multiple inputs," Proc. IEEE, vol. 62, pp. 1088-1119, August 1974.
[23] Burton S. Abrams, "Making nonlinear interference rejection work in QPSK-SS receivers," in Conf. Record, IEEE Milcom 95, pp. 774-777, San Diego CA, Nov. 6-8, 1995.
[24] R.G. Harrison, "Theory of the varactor frequency halver," IEEE MTT Symposium Digest, pp. 203-205, Boston, June 1983.
[25] R.G. Harrison, "Theoretical and experimental studies on frequency division at microwave and millimetre frequencies, vol. II: Theory of broadband abrupt-junction and Schottky-barrier frequency halvers," Carleton Electronics Research Laboratory Tech. Rept. No. CERL-85-3, DND/DSS contract no. 8SU81-00006, March 1985.
[26] Inder Bahl, and Prakash Bhartia, *Microwave Solid State Circuit Design*, John Wiley & Sons, New York, 1988.
[27] W.B. Davenport and W.L. Root, *An Introduction to the Theory of Random Signals and Noise*, McGraw-Hill, New York, 1958.

UNCLASSIFIED

SECURITY CLASSIFICATION OF FORM
(highest classification of Title, Abstract, Keywords)

DOCUMENT CONTROL DATA

(Security classification of title, body of abstract and indexing annotation must be entered when the overall document is classified)

1. **ORIGINATOR** (the name and address of the organization preparing the document. Organizations for whom the document was prepared, e.g. Establishment sponsoring a contractor's report, or tasking agency, are entered in section 8.)
Communications Research Centre,
Shirley's Bay, Ottawa

2. **SECURITY CLASSIFICATION** (overall security classification of the document including special warning terms if applicable)
UNCLASSIFIED

3. **TITLE** (the complete document title as indicated on the title page. Its classification should be indicated by the appropriate abbreviation (S,C or U) in parentheses after the title.)
Analysis and Experiments on the Frequency Independent Strong Signal Suppressor (FISSS) (U)

4. **AUTHORS** (Last name, first name, middle initial)
D. Sychaleun (CRC), E.B. Felstead (CRC), G.A. Morin (DREO)

5. **DATE OF PUBLICATION** (month and year of publication of document)
Nov. 1998

6a. **NO. OF PAGES** (total containing information. Include Annexes, Appendices, etc.)
viii + 48

6b. **NO. OF REFS** (total cited in document)
27

7. **DESCRIPTIVE NOTES** (the category of the document, e.g. technical report, technical note or memorandum. If appropriate, enter the type of report, e.g. interim, progress, summary, annual or final. Give the inclusive dates when a specific reporting period is covered.)
CRC Report

8. **SPONSORING ACTIVITY** (the name of the department project office or laboratory sponsoring the research and development. Include the address.)
Defence Research Establishment Ottawa,
3701 Carling Ave., Ottawa, ON, CANADA, K1A 0Z4

9a. **PROJECT OR GRANT NO.** (if appropriate, the applicable research and development project or grant number under which the document was written. Please specify whether project or grant)
5ca14

9b. **CONTRACT NO.** (if appropriate, the applicable number under which the document was written)

10a. **ORIGINATOR'S DOCUMENT NUMBER** (the official document number by which the document is identified by the originating activity. This number must be unique to this document.)
CRC Report # CRC-RP-98-006

10b. **OTHER DOCUMENT NOS.** (Any other numbers which may be assigned this document either by the originator or by the sponsor)

11. **DOCUMENT AVAILABILITY** (any limitations on further dissemination of the document, other than those imposed by security classification)

(X) Unlimited distribution
( ) Distribution limited to defence departments and defence contractors; further distribution only as approved
( ) Distribution limited to defence departments and Canadian defence contractors; further distribution only as approved
( ) Distribution limited to government departments and agencies; further distribution only as approved
( ) Distribution limited to defence departments; further distribution only as approved
( ) Other (please specify):

12. **DOCUMENT ANNOUNCEMENT** (any limitation to the bibliographic announcement of this document. This will normally correspond to the Document Availability (11). however, where further distribution (beyond the audience specified in 11) is possible, a wider announcement audience may be selected.)
Unlimited Announcement

UNCLASSIFIED

SECURITY CLASSIFICATION OF FORM

13. **ABSTRACT** (a brief and factual summary of the document. It may also appear elsewhere in the body of the document itself. It is highly desirable that the abstract of classified documents be unclassified. Each paragraph of the abstract shall begin with an indication of the security classification of the information in the paragraph (unless the document itself is unclassified) represented as (S), (C), or (U). It is not necessary to include here abstracts in both official languages unless the text is bilingual).

The frequency-independent strong-signal suppressor (FISSS) uses nonlinear processing plus cancellation techniques to provide substantial interference suppression. However, only laboratory proof of its operation existed. Although considerable effort went into trying to determine the principle of operation, this principle was not found. In this report, some analytical and simulation attacks on this problem are described. Extensive laboratory measurements were made on devices operating at 1.5 GHz and 10 GHz. The 10 GHz device was combined with direct-sequence spread spectrum, and had measured processing gains of about 12 dB against CW and frequency-modulated single tones. The experimental highlight was the successful suppression of noise interference of between 6 and 12 dB, depending upon the noise bandwidth.

14. **KEYWORDS, DESCRIPTORS or IDENTIFIERS** (technically meaningful terms or short phrases that characterize a document and could be helpful in cataloguing the document. They should be selected so that no security classification is required. Identifiers, such as equipment model designation, trade name, military project code name, geographic location may also be included. If possible keywords should be selected from a published thesaurus. e.g. Thesaurus of Engineering and Scientific Terms (TEST) and that thesaurus-identified. If it is not possible to select indexing terms which are Unclassified, the classification of each should be indicated as with the title.)

frequency independent strong signal suppressor
FISSS
nonlinear anti-jamming

INDUSTRY CANADA / INDUSTRIE CANADA
208902